Cureus
Part of SPRINGER NATURE

Open Access Review Article

Contrast-Enhanced Ultrasound Versus CT/MRI for the Characterization of Focal Liver Lesions: A Systematic Review and Meta-Analysis

Review began 11/02/2026
Review ended 11/14/2026
Published 11/19/2026

© **Copyright** 2026
Elazomy et al. This is an open access article distributed under the terms of the Creative Commons Attribution License CC-BY 4.0., which permits unrestricted use, distribution, and reproduction in any medium, provided the original author and source are credited.

DOI: 10.7759/cureus.119954

Mohamed R. Elazomy [1], Wedad A. Kaabi [2], Aesha A. Hassan [3], Shahad F. Bagdood [4], Sheikhah Binmahfooz [4], Ahmed M. Alzahrani [5], Norah M. Almarzouq [6], Abdullah Alhussain [7], Yazan Daghriri [8], Layan T. Aldhowayan [9], Ahad Alhazmi [10], Abdulmalik Meri [11], Alanood M. Hakami [8], Dina M. Almasoudi [12], Salma A. Tahiri [13]

1. Department of Radiology, Academic Medical City, Imam Abdulrahman Bin Faisal University, Al Khobar, SAU 2. Department of Radiology, Meena Health Company, Riyadh, SAU 3. Department of Radiology, Al Noor Specialist Hospital, Makkah, SAU 4. Department of Medicine and Surgery, Fakeeh College for Medical Sciences, Makkah, SAU 5. College of Medicine, Al-Baha University, Al-Baha, SAU 6. Department of Nuclear Medicine, Saudi Society of Nuclear Medicine and Molecular Imaging, Riyadh, SAU 7. Unaizah College of Medicine, Qassim University, Buraidah, SAU 8. College of Medicine, Jazan University, Jazan, SAU 9. College of Medicine, Qassim University, Buraidah, SAU 10. College of Medicine and Medical Science, Arabian Gulf University, Manama, BHR 11. Department of Internal Medicine, Ministry of Health (MOH) - Aseer Region, Abha, SAU 12. College of Medicine, Dar Al Uloom University, Riyadh, SAU 13. Department of Radiological Technology, Jazan University, Jazan, SAU

Corresponding author: Mohamed R. Elazomy, dr.mohamed.elazomy@outlook.com

Abstract

Contrast-enhanced ultrasound (CEUS) has emerged as a non-invasive, radiation-free alternative to multiphasic computed tomography (CT) and magnetic resonance imaging (MRI) for characterizing focal liver lesions (FLLs). However, primary studies report heterogeneous diagnostic accuracy, necessitating an updated quantitative synthesis to establish the comparative effectiveness of CEUS.

This systematic review and meta-analysis was conducted following the Preferred Reporting Items for Systematic Reviews and Meta-Analyses extension for Diagnostic Test Accuracy (PRISMA-DTA) guidelines and registered in the International Prospective Register of Systematic Reviews (PROSPERO) (CRD420261344025). A search of major databases was performed up to August 2026 for studies directly comparing CEUS with CT and/or MRI for FLL characterization. Quality assessment was conducted using the Quality Assessment of Diagnostic Accuracy Studies 2 (QUADAS-2). Pooled sensitivity, specificity, and area under the curve (AUC) were calculated using a hierarchical bivariate random-effects model and hierarchical summary receiver operating characteristic (HSROC) models.

Thirty-one studies were included, with 28 contributing to the quantitative synthesis (60 study arms). CEUS demonstrated an overall pooled sensitivity of 86.2% (95% confidence interval {CI}: 80.6%-90.4%) and specificity of 90.2% (95% CI: 86.6%-92.9%), with an AUC of 0.926, compared with 0.895 for CT and 0.914 for MRI. In head-to-head comparisons, there was no statistically significant difference in sensitivity or specificity between CEUS and CT (p_{sens} = 0.812; p_{spec} = 0.504) or MRI (p_{sens} = 0.977; p_{spec} = 0.962). CEUS performed comparably to CT/MRI for hepatocellular carcinoma (HCC) characterization and showed numerically higher sensitivity for liver metastases. Subgroup analyses showed lower CEUS sensitivity for HCC-specific diagnosis than for overall malignancy and in cirrhotic/at-risk cohorts. The overall certainty of evidence was graded as low according to the Grading of Recommendations Assessment, Development, and Evaluation (GRADE) framework.

CEUS provides high diagnostic accuracy for FLL characterization, without statistically significant differences from contrast-enhanced computed tomography (CECT) and contrast-enhanced magnetic resonance imaging (CEMRI). Given the low certainty of the evidence and its lower sensitivity for HCC-specific diagnosis and small nodules, CEUS is best used as a complementary, problem-solving modality, particularly when radiation exposure or CT/MRI contrast agents should be avoided.

Categories: Radiology, Oncology, Gastroenterology
Keywords: computed tomography, contrast-enhanced ultrasound, diagnostic accuracy, focal liver lesions, hepatocellular carcinoma, magnetic resonance imaging, meta-analysis

Introduction And Background

Focal liver lesions (FLLs) encompass a diverse and heterogeneous spectrum of hepatic abnormalities, ranging from benign entities, such as hemangiomas, focal nodular hyperplasia (FNH), simple cysts, and hepatic adenomas, to malignant diseases, primarily hepatocellular carcinoma (HCC) and metastatic liver deposits [1,2]. The incidental detection of FLLs has surged in recent years due to the utilization of routine

abdominal imaging and global screening programs for populations with chronic liver disease [3]. The accurate and timely characterization of these lesions is of clinical importance, as it dictates therapeutic decision-making, patient prognostication, and the avoidance of unnecessary invasive procedures or patient anxiety associated with ambiguous diagnoses [4,5].

Conventional B-mode and color Doppler ultrasound (US) serve as the established first-line modalities for evaluating the liver due to their low cost, widespread accessibility, and lack of ionizing radiation [4]. However, conventional US suffers from limited diagnostic specificity, as many benign and malignant lesions share overlapping morphological and echogenic features [4,5]. Multiphasic contrast-enhanced computed tomography (CECT) and contrast-enhanced magnetic resonance imaging (CEMRI) have been relied upon as the reference cross-sectional imaging standards for definitive FLL characterization [3]. Despite their high diagnostic accuracy, CECT and CEMRI are constrained by several limitations, including exposure to ionizing radiation (with CECT), high procedural costs, limited accessibility, and the requirement for potentially nephrotoxic or hepatotoxic contrast agents [6]. Furthermore, contraindications, such as severe renal insufficiency, claustrophobia, iodine allergies, or the presence of metallic implants, often preclude their use in a proportion of patients [5,7].

Contrast-enhanced ultrasound (CEUS) has emerged as a powerful, non-invasive alternative for the characterization of hepatic lesions [6,8]. Utilizing second-generation microbubble contrast agents, such as sulfur hexafluoride (SonoVue®/Lumason®), CEUS facilitates the continuous, real-time dynamic assessment of lesion microcirculation and vascularity across the arterial, portal-venous, and late parenchymal phases [6,8]. This real-time capability overcomes the temporal snapshot limitations of CECT and CEMRI, allowing for the precise capture of transient hypervascularity and subsequent washout patterns critical for differentiating benign from malignant tissues [6,9]. Moreover, microbubble agents are purely intravascular blood-pool tracers whose gas component is eliminated via the lungs; they are not nephrotoxic and do not require the assessment of renal function, which makes them suitable for patients with renal impairment, and sulfur hexafluoride microbubbles are also approved for pediatric liver imaging [8,10]. Nevertheless, CEUS is not free of risk: Rare serious hypersensitivity and cardiopulmonary reactions have been reported, agent-specific regulatory labeling lists contraindications and precautions that differ between agents and jurisdictions, and safety during pregnancy has not been established, so use in pregnant women should follow the applicable regulatory guidance and an individual risk-benefit assessment.

The diagnostic utility of CEUS has been recognized and standardized globally, culminating in endorsements by international guidelines, including those of the European Federation of Societies for Ultrasound in Medicine and Biology (EFSUMB), the World Federation for Ultrasound in Medicine and Biology (WFUMB), and the formalization of the CEUS Liver Imaging Reporting and Data System (LI-RADS) by the American College of Radiology (ACR) [4,5].

Despite growing international consensus, primary studies evaluating the diagnostic accuracy of CEUS relative to computed tomography (CT) and magnetic resonance imaging (MRI) report varying and sometimes heterogeneous findings [11-13]. Diagnostic performance fluctuates based on variables such as lesion size (e.g., subcentimeter lesions), underlying parenchymal disease (cirrhotic versus non-cirrhotic livers), and operator experience [5,10]. While previous systematic reviews and meta-analyses have evaluated these modalities, the continuous evolution of contrast-specific ultrasound software and the expanding clinical footprint of CEUS necessitate an updated quantitative synthesis [3,9].

Therefore, this systematic review and meta-analysis aimed to evaluate and quantitatively synthesize the evidence comparing the diagnostic accuracy of contrast-enhanced ultrasound with computed tomography (CT) and/or magnetic resonance imaging (MRI) for the characterization of focal liver lesions. By determining pooled performance metrics, including sensitivity, specificity, positive predictive value (PPV) and negative predictive value (NPV), and overall diagnostic accuracy, this study seeks to assess the comparative effectiveness of CEUS in differentiating benign from malignant hepatic lesions, thereby informing evidence-based imaging strategies and optimizing future clinical guidelines.

Review

Methods

Protocol Registration and Reporting Standards

This systematic review and meta-analysis was conducted in accordance with the Preferred Reporting Items for Systematic Reviews and Meta-Analyses (PRISMA) 2020 statement [14], alongside the PRISMA extension for Diagnostic Test Accuracy (PRISMA-DTA) guidelines [15]. The study protocol was prospectively registered in the International Prospective Register of Systematic Reviews (PROSPERO; registration number: CRD420261344025). Methodological procedures adhered to the recommendations outlined in the Cochrane Handbook for Systematic Reviews of Diagnostic Test Accuracy [16].

Search Strategy and Information Sources

A systematic literature search was performed across major electronic databases, including PubMed/Medical Literature Analysis and Retrieval System Online (MEDLINE), Embase, Cochrane Central Register of Controlled Trials (CENTRAL), Scopus, and Web of Science, from their inception to August 2026. To minimize language and publication biases, no language or publication date restrictions were applied. The search syntax was constructed using a combination of Medical Subject Headings (MeSH/Emtree) and free-text keywords optimized with Boolean operators (AND/OR/NOT) and truncations. Search domains encompassed combinations of terms related to the index test (e.g., "contrast-enhanced ultrasound," "CEUS," "SonoVue," "Lumason," and "microbubbles"), the comparators (e.g., "computed tomography," "magnetic resonance imaging," "CECT," and "CEMRI"), and the target conditions (e.g., "focal liver lesions," "hepatocellular carcinoma," "liver metastasis," and "hepatic adenoma"). To ensure literature saturation, the backward and forward citation tracking ("snowballing") of the included studies and relevant review articles was conducted, supplemented by a grey literature search of ClinicalTrials.gov and the World Health Organization International Clinical Trials Registry Platform (WHO-ICTRP). The complete database-specific search strategies are presented in the Appendices.

Eligibility Criteria

Studies were selected based on pre-defined inclusion criteria structured around the population, index test/exposure, comparator, outcome, and study design (PI/ECOS) framework for diagnostic accuracy [16]. The population included adult or pediatric patients presenting with one or more focal liver lesions (e.g., benign or malignant, including HCC, metastases, hemangioma, and FNH) requiring diagnostic imaging evaluation.

The index test was CEUS utilizing commercially approved second-generation ultrasound contrast agents (e.g., sulfur hexafluoride). The comparator was multiphasic CECT and/or CEMRI, utilizing either extracellular or hepatobiliary-specific contrast agents, and the reference standard was histopathological examination (via biopsy or surgical resection) or a composite clinical/radiological reference standard as defined below.

A composite reference standard was accepted when lesions without histological confirmation were classified by typical features on a reference cross-sectional examination (for benign entities such as hemangioma and FNH); by the consensus review of all available imaging, clinical, and laboratory information; and/or by imaging follow-up showing stability, regression, or interval growth or change in enhancement. The minimum follow-up was that specified by each primary study; where reported, it ranged from six months to two years. The components of the reference standard, the proportion of histologically verified lesions, and whether the index test or the comparator contributed to the final diagnosis were extracted independently by two reviewers, and disagreements were adjudicated by a third reviewer. Studies in which the comparator imaging formed part of the reference standard (incorporation bias) or in which only a subset of lesions received histological verification (differential verification) were rated accordingly in the reference standard and flow-and-timing domains of the Quality Assessment of Diagnostic Accuracy Studies 2 (QUADAS-2), and their influence was examined in a sensitivity analysis restricted to studies with a histological reference standard.

Studies must have reported sufficient raw data, specifically true positive (TP), false positive (FP), true negative (TN), and false negative (FN) values, to reconstruct 2 × 2 contingency tables for diagnostic performance. Prospective and retrospective cross-sectional diagnostic accuracy studies, cohort studies, and randomized trials were included.

The exclusion criteria were as follows: (1) studies evaluating diffuse liver diseases without focal lesions, (2) fundamental animal or in vitro models, (3) studies focusing on unenhanced B-mode or Doppler ultrasound without contrast enhancement, and (4) case reports, editorials, narrative reviews, and case series containing fewer than 10 patients.

Study Selection and Data Extraction

All retrieved citations were imported into reference management software to remove duplicates. Two investigators independently screened the titles and abstracts, followed by a full-text review of potentially eligible manuscripts. Inter-rater reliability (IRR) for study inclusion was quantified using Cohen's kappa coefficient (κ) [17]. Disagreements were resolved through adjudication by a third reviewer.

Data extraction was independently performed using a standardized, piloted form. The extracted variables included study characteristics (author, year, country, and design), patient demographics (age, sex, and underlying liver disease/cirrhosis status), technical parameters (contrast agent type, imaging protocols, and blinding status), and raw diagnostic metrics (TP, FP, TN, and FN) on a per-patient or per-lesion basis, as reported. The positive-test definition applied in each study and the extracted 2 × 2 tables for every study and imaging modality are presented in the Appendices. Each study contributed one 2 × 2 table per imaging test, using the unit of analysis of the primary study (per-lesion in 21 studies and per-patient in seven studies). When patients had more than one lesion, lesion-level counts were analyzed as reported, and the influence of

the unit of analysis was examined by meta-regression and by a sensitivity analysis restricted to per-lesion data.

Quality Assessment and Risk of Bias (RoB)

The methodological quality and risk of bias (RoB) of the included studies were evaluated using the Quality Assessment of Diagnostic Accuracy Studies 2 (QUADAS-2) tool [18]. Two reviewers independently assessed four key domains: patient selection, index test, reference standard, and flow and timing. Each domain was judged as having a low, high, or unclear risk of bias, alongside an evaluation of applicability concerns regarding the patient cohort, index test, and reference standard.

Statistical Analysis and Data Synthesis

All statistical analyses and data visualizations were executed using R software version 4.6.1 (R Foundation for Statistical Computing, Vienna, Austria), employing the mada, meta, and lme4 packages [19].

Because sensitivity and specificity in diagnostic studies are interdependent and subject to threshold effects, classical univariate pooling methods are inadequate. Therefore, pooled estimates of sensitivity, specificity, positive likelihood ratio (PLR), negative likelihood ratio (NLR), and diagnostic odds ratio (DOR) were calculated using a hierarchical bivariate random-effects model [20]. The hierarchical summary receiver operating characteristic (HSROC) model was utilized to plot summary curves and calculate the area under the curve (AUC), serving as a global metric of diagnostic performance [21].

Positivity thresholds were not uniform across studies and were therefore harmonized according to the target condition. In HCC-focused studies, a positive index or comparator test was the study-defined non-invasive HCC criterion (arterial-phase hyperenhancement, followed by washout, American Association for the Study of Liver Diseases {AASLD}/European Association for the Study of the Liver {EASL} criteria, or the LR-5 category of CEUS or CT/MRI LI-RADS); in studies differentiating malignant from benign lesions, a positive test was the classification of the lesion as malignant; and in metastasis-focused studies, a positive test was the characterization of the lesion as a metastasis. Indeterminate results were counted as incorrect classifications where the primary study did so. Because HCC-specific diagnosis and benign-versus-malignant differentiation are distinct diagnostic endpoints, target condition was a pre-specified covariate, and HCC- and metastasis-specific accuracy was pooled separately.

Comparative accuracy was estimated only from studies in which CEUS and the comparator were performed in the same patients (head-to-head comparisons). A bivariate binomial-normal meta-regression with test type (CEUS versus comparator) as a covariate on logit sensitivity and logit specificity was fitted, in which each test arm was entered with its own random effects. For the study that reported CT and MRI results in different patient subsets, the CEUS results of the full cohort were compared with each subset. In the comparison with any CT/MRI, the four studies reporting both CT and MRI contributed one CEUS arm and two comparator arms. Differences between tests are expressed as relative odds of sensitivity and specificity (comparator versus CEUS) with 95% confidence intervals (CIs) and were tested with likelihood-ratio tests for sensitivity, specificity, and both jointly. AUCs are reported with 95% CIs obtained from 1,000 study-level bootstrap resamples.

Heterogeneity Assessment and Exploration

Inter-study heterogeneity was quantified using the I^2 statistic, Cochran's Q test, and the between-study variance parameter tau-squared (τ^2) [22]. Substantial heterogeneity ($I^2 > 50\%$ or $p < 0.10$ for the Q test) was explored through subgroup analyses and univariate meta-regression. Pre-specified covariates included underlying liver status (cirrhotic versus non-cirrhotic), lesion size (studies restricted to small nodules of ⩽20-30 mm versus unrestricted size and ⩽20 mm strata where reported), lesion etiology (HCC versus metastasis versus benign), comparator modality (CECT versus CEMRI), and blinding status. To assess confounding between correlated covariates, target condition, liver background, and lesion-size restriction were also entered simultaneously in a multivariable bivariate meta-regression. Sensitivity analyses using a leave-one-out approach were conducted to test the robustness of the pooled estimates.

Publication Bias and Clinical Utility

Publication bias and small-study effects were evaluated visually via contour-enhanced funnel plots and statistically confirmed using Deeks' funnel plot asymmetry test, where a p-value of <0.10 signifies significant publication bias [23]. To contextualize the clinical relevance of CEUS, Fagan's nomogram was constructed to visualize the pre-test to post-test probability shifts based on the pooled PLR and NLR [24]. Post-test probabilities were additionally calculated at pre-test probabilities of 10%, 25%, 50%, and 75% to reflect lower-prevalence settings, such as incidentally detected lesions. The negative predictive value (NPV) was calculated as one minus the post-test probability after a negative result.

Certainty of Evidence

The overall certainty of the evidence was graded using the Grading of Recommendations Assessment, Development, and Evaluation (GRADE) framework adapted for Diagnostic Test Accuracy (GRADE-DTA) [25]. Evidence was downgraded based on the severity of study limitations (risk of bias), indirectness, inconsistency, imprecision, and publication bias, culminating in a summary of findings table indicating high, moderate, low, or very low certainty of evidence.

Results

Literature Search and Study Selection

A systematic literature search across major electronic databases and trial registries yielded 1,197 records. After the removal of 219 duplicates, 978 records underwent title and abstract screening, leading to the exclusion of 919 studies. Fifty-nine full-text reports were sought and retrieved for eligibility assessment. Of these, 28 reports were excluded for reasons including the lack of an appropriate comparator (n = 9), incorrect intervention (n = 8), insufficient sample size (case series <10 patients; n = 6), review article design (n = 3), and insufficient diagnostic data to construct 2 × 2 contingency tables (n = 2). Thirty-one studies were included in the qualitative synthesis [26-56], of which 28 contributed data to the primary quantitative meta-analysis [26-53]. The study selection process is detailed in Figure *1*. Three studies did not provide a CEUS-alone 2 × 2 table for the pooled endpoints and were therefore not included in the primary meta-analysis: One reported only four malignant lesions but provided lesion-specific data for hemangioma and FNH, which were used in the lesion-specific analysis and assessed with QUADAS-2 [54]; one reported sensitivity and specificity only for subgroups without denominators [55]; and one evaluated CEUS only as a second-line test added to CT/MRI LI-RADS, without stand-alone CEUS results [56].

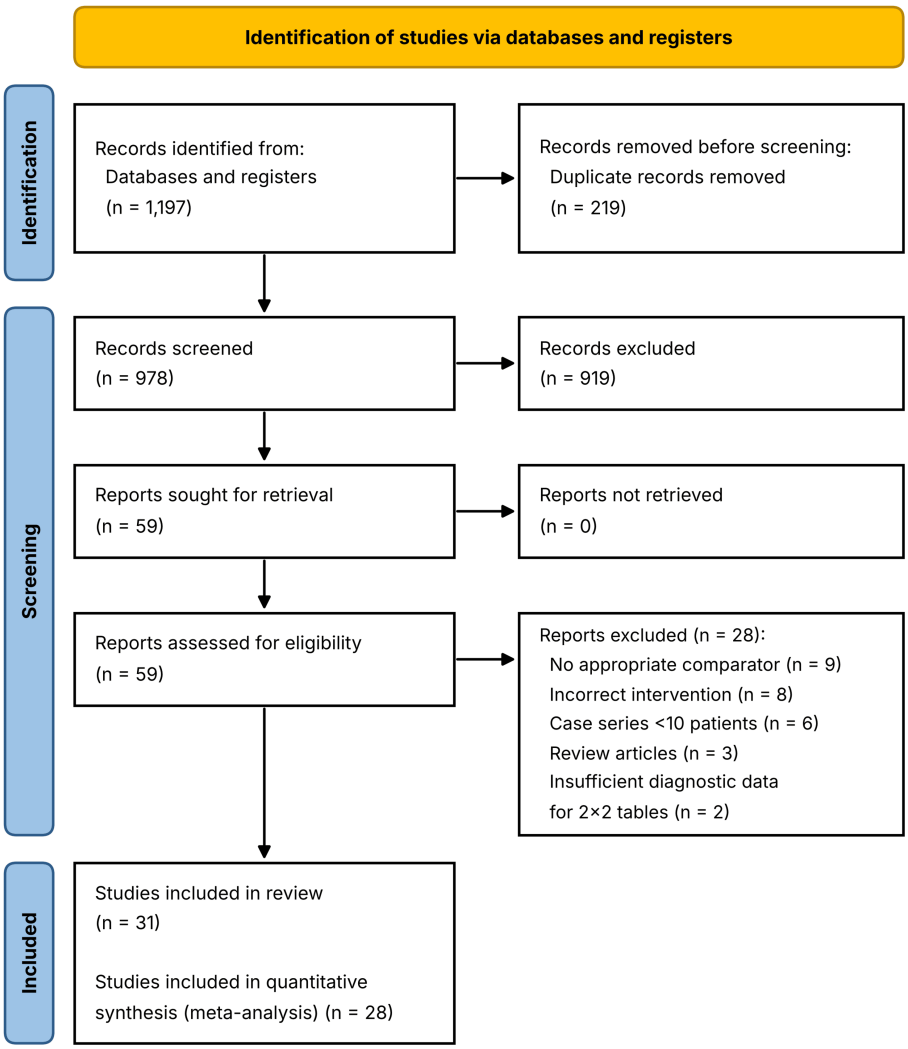


FIGURE 1: PRISMA 2020 flow diagram.

Flow diagram of study identification, screening, and inclusion, following the PRISMA 2020 statement [14].

PRISMA: Preferred Reporting Items for Systematic Reviews and Meta-Analyses

Characteristics of Included Studies

The baseline characteristics of the 28 included studies are summarized in Table *1*. The studies were published between 2006 and 2025 [26-53] and comprised 18 prospective [29,30,32-42,44,49-51,53] and 10 retrospective or cross-sectional designs [26-28,31,43,45-48,52]. The studies were widely distributed, including cohorts from China [26,31,36,37,52], Italy [28,29,41,42,49,51], Germany [32,33,35,43,48], Japan [30,38], Spain [34,50], Canada [39,40], France [44], South Korea [47], Switzerland [45], Romania [27], India [46], and Egypt [53]. The reference standard was histopathology alone [29-34,36,37,41,43,46,51,52] or a composite of histopathology and imaging follow-up [26-28,35,38-40,42,44,45,47-50,53]. Sulfur hexafluoride (SonoVue) was the predominant contrast agent utilized for CEUS (n = 24) [26-29,31-37,41-53], followed by perfluorobutane (Sonazoid®; n = 2) [30,38] and perflutren (Definity®; n = 2) [39,40]. The blinded reading of imaging modalities was confirmed in most of the studies (n = 17) [26,29-31,34-37,39-43,49-52], while it was absent or unclear in 11 studies [27,28,32,33,38,44-48,53]. The target conditions evaluated included HCC (n = 10) [26,27,29-31,34,36,41,42,52], liver metastases (n = 2) [38,49], and overall focal liver malignancy (n = 16) [28,32,33,35,37,39,40,43-48,50,51,53]. In the two reports from the same German multicenter (Deutsche Gesellschaft für Ultraschall in der Medizin {DEGUM}) cohort, 269 and 267 patients underwent CEUS with MRI and CT, respectively, but diagnostic accuracy was reported only for the histologically verified subgroups (82 and 158 patients), which were therefore used in this meta-analysis (Table *1*) [32,33]; possible overlap between these reports was examined in a sensitivity analysis excluding the study by Seitz et al. [32].

			Patients	Mean age	Male	Liver	Size group	Mean size	Contrast	Agent	Target	Reference	Unit of

Study and reference	Country	Design	(n)	(years)	(%)	background	(mm)	(mm)	agent	class	condition	standard	analysis
Li et al., 2025 [26]	China	Retrospective analysis of prospective cohort	281	55	84.3	Cirrhotic	Any	40	SonoVue	SHF	HCC	Composite	Lesion
Dumitrescu et al., 2013 [27]	Romania	Retrospective	126	59	59.5	Mixed	Any	52	SonoVue	SHF	HCC	Composite	Patient
D'Onofrio et al., 2014 [28]	Italy	Retrospective	147	59.4	63.3	Mixed	Any	NR	SonoVue	SHF	Malignancy	Composite	Lesion
Giorgio et al., 2007 [29]	Italy	Prospective	73	63	67.1	Cirrhotic	≤30	NR	SonoVue	SHF	HCC	Histology	Lesion
Takahashi et al., 2013 [30]	Japan	Prospective	56	NR	71.4	Cirrhotic	≤30	17.5	Sonazoid	PFB	HCC	Histology	Lesion
Wang et al., 2020 [31]	China	Retrospective	63	56	74.6	Cirrhotic	Any	35	SonoVue	SHF	HCC	Histology	Lesion
Seitz et al., 2010 [32]	Germany	Prospective	269 (82)	59.6	63.1	Mixed	Any	NR	SonoVue	SHF	Malignancy	Histology	Lesion
Seitz et al., 2009 [33]	Germany	Prospective	267 (158)	NR	NR	Mixed	Any	NR	SonoVue	SHF	Malignancy	Histology	Lesion
Forner et al., 2008 [34]	Spain	Prospective	89	65	59.6	Cirrhotic	≤20	14	SonoVue	SHF	HCC	Histology	Lesion
Clevert et al., 2009 [35]	Germany	Prospective	100	57	57	Mixed	Any	NR	SonoVue	SHF	Malignancy	Composite	Patient
Dai et al., 2008 [36]	China	Prospective	72	NR	NR	Cirrhotic	≤20	NR	SonoVue	SHF	HCC	Histology	Lesion
Li et al., 2007 [37]	China	Prospective	109	46	66.1	Mixed	Any	29	SonoVue	SHF	Malignancy	Histology	Lesion
Shiozawa et al., 2017 [38]	Japan	Prospective	69	66	66.7	Non-cirrhotic	Any	21	Sonazoid	PFB	Metastasis	Composite	Lesion
Burrowes et al., 2021 [39]	Canada	Prospective	214	57	43.5	Mixed	Any	NR	Definity	Perflutren	Malignancy	Composite	Lesion
Hu et al., 2023 [40]	Canada	Prospective	195	NR	NR	Cirrhotic	Any	NR	Definity	Perflutren	Malignancy	Composite	Patient
Sangiovanni et al., 2010 [41]	Italy	Prospective	64	65	73	Cirrhotic	≤20	NR	SonoVue	SHF	HCC	Histology	Lesion
Leoni et al., 2010 [42]	Italy	Prospective	60	65	86.7	Cirrhotic	≤30	NR	SonoVue	SHF	HCC	Composite	Lesion
Blondin et al., 2011 [43]	Germany	Retrospective	33	63.2	75.8	Cirrhotic	Any	NR	SonoVue	SHF	Malignancy	Histology	Lesion
Trillaud et al., 2009 [44]	France	Prospective	134	55.3	47.5	Mixed	Any	NR	SonoVue	SHF	Malignancy	Composite	Patient
Sawatzki et al., 2019 [45]	Switzerland	Retrospective	112	NR	NR	Mixed	Any	NR	SonoVue	SHF	Malignancy	Composite	Patient
Gnanasigamani et al., 2020 [46]	India	Cross-sectional	51	NR	NR	Mixed	Any	NR	SonoVue	SHF	Malignancy	Histology	Patient
Ryu et al., 2014 [47]	South Korea	Retrospective	48	58	77.1	Mixed	Any	NR	SonoVue	SHF	Malignancy	Composite	Lesion
Beyer et al., 2017 [48]	Germany	Retrospective	83	59.8	71.1	Mixed	Any	NR	SonoVue	SHF	Malignancy	Composite	Patient
Quaia et al., 2006 [49]	Italy	Prospective	73	57	54.5	Non-cirrhotic	Any	NR	SonoVue	SHF	Metastasis	Composite	Lesion
Catala et al., 2007 [50]	Spain	Prospective	77	62	58.4	Mixed	Any	NR	SonoVue	SHF	Malignancy	Composite	Lesion
Quaia et al., 2009 [51]	Italy	Prospective	106	70	64.2	Cirrhotic	Any	NR	SonoVue	SHF	Malignancy	Histology	Lesion
Ding et al., 2021 [52]	China	Retrospective	239	59.1	NR	Cirrhotic	Any	NR	SonoVue	SHF	HCC	Histology	Lesion
Mansour et al., 2021 [53]	Egypt	Prospective	60	53.8	63.3	Mixed	Any	28	SonoVue	SHF	Malignancy	Composite	Lesion

TABLE 1: Characteristics of the 28 studies included in the quantitative synthesis.

Size group: upper lesion-size limit for enrolment (any = unrestricted). Composite reference standard: histology and/or imaging follow-up. For the two DEGUM multicenter reports (Seitz et al., 2010 [32]; Seitz et al., 2009 [33]), the number of patients who underwent both CEUS and the comparator is followed, in parentheses, by the number in the histologically verified subgroup used for the accuracy analysis.

CEUS, contrast-enhanced ultrasound; HCC, hepatocellular carcinoma; SHF, sulfur hexafluoride; PFB, perfluorobutane; NR, not reported

Methodological Quality and Risk of Bias

The methodological quality of the included studies, assessed via the QUADAS-2 tool, is visualized in the traffic-light plot (Figure *2*) and summarized as domain proportions (Figure *3*). The overall risk of bias was low or unclear across most domains. A high risk of bias was noted in the patient selection domain in a minority of studies, due to retrospective designs or exclusion of non-visualized lesions [30,31,39,43,48,52]. The reference standard domain exhibited low risk of bias in studies utilizing universal histopathology but was rated unclear or high in studies relying on composite imaging references with differential verification, with a high risk of bias in seven studies [27,35,39,44,45,47,53]. Applicability concerns were low in most studies, with high concern in three [28,30,48].

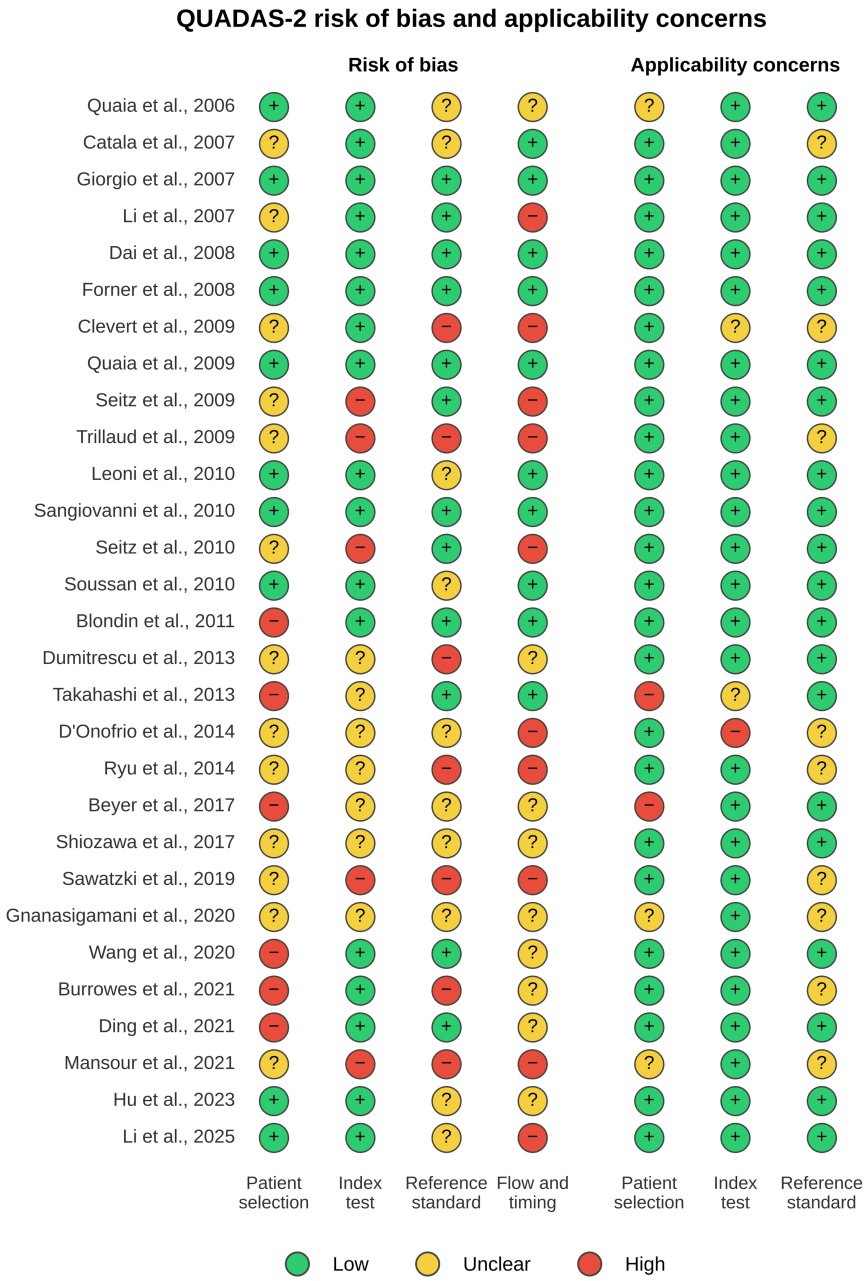


FIGURE 2: QUADAS-2 risk of bias traffic-light plot of per-study judgments.

Per-study judgments for the 28 studies included in the quantitative synthesis [26-53] and the study that contributed lesion-specific data only [54]. Green (+), low; yellow (?), unclear; and red (-), high risk of bias or high concern regarding applicability [18].

QUADAS-2: Quality Assessment of Diagnostic Accuracy Studies 2

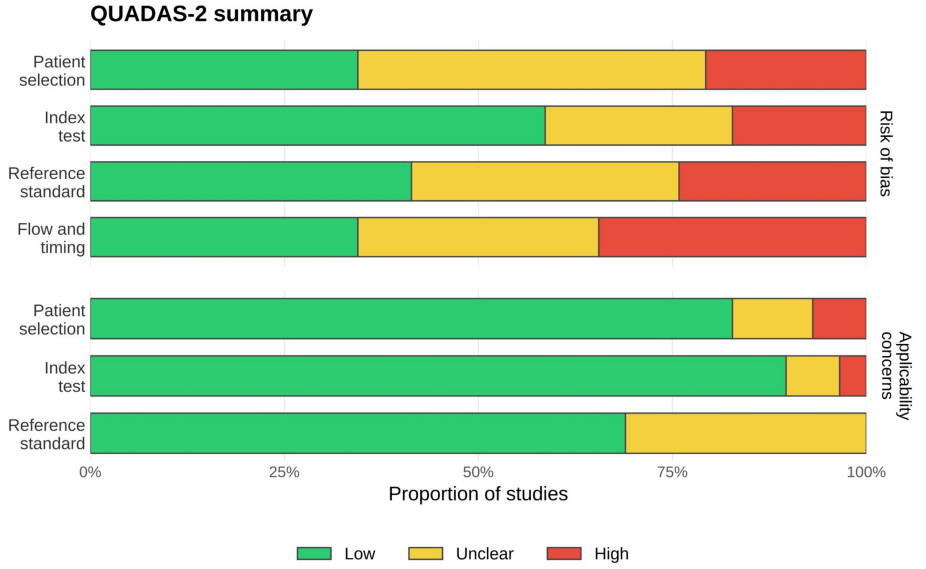


FIGURE 3: QUADAS-2 risk of bias: proportion of studies rated low, unclear, or high in each domain.

Proportion of the included studies [26-54] judged at low, unclear, or high risk of bias (upper panel) and with low, unclear, or high concern regarding applicability (lower panel) in each QUADAS-2 domain [18].

QUADAS-2: Quality Assessment of Diagnostic Accuracy Studies 2

Overall Diagnostic Accuracy

Data from 60 study arms (28 CEUS [26-53], 13 CT [33,35-37,39,41,42,46,47,49-51,53], 15 MRI [27-32,34,38-43,47,48], and four mixed CT/MRI [26,44,45,52]) were extracted for pooled analysis. Using a hierarchical bivariate random-effects model, CEUS demonstrated an overall pooled sensitivity of 86.2% (95% CI: 80.6%-90.4%) and specificity of 90.2% (95% CI: 86.6%-92.9%). By comparison, the pooled sensitivity and specificity for CT were 86.5% (95% CI: 78.2%-91.9%) and 86.6% (95% CI: 78.0%-92.2%), respectively, while MRI yielded a sensitivity of 81.7% (95% CI: 72.4%-88.3%) and a specificity of 91.8% (95% CI: 84.7%-95.8%). The diagnostic odds ratio (DOR) for CEUS was 57.7 (95% CI: 39.2-84.8), compared with 41.4 (95% CI: 22.6-75.7) for CT and 49.9 (95% CI: 26.8-93.0) for MRI. The AUC derived from the HSROC models was 0.926 (95% CI: 0.909-0.941) for CEUS, 0.895 (95% CI: 0.767-0.928) for CT, and 0.914 (95% CI: 0.877-0.941) for MRI, with overlapping confidence intervals (Figures 4-6); because these estimates were derived from separate models, comparisons between tests are based on the head-to-head analyses below.

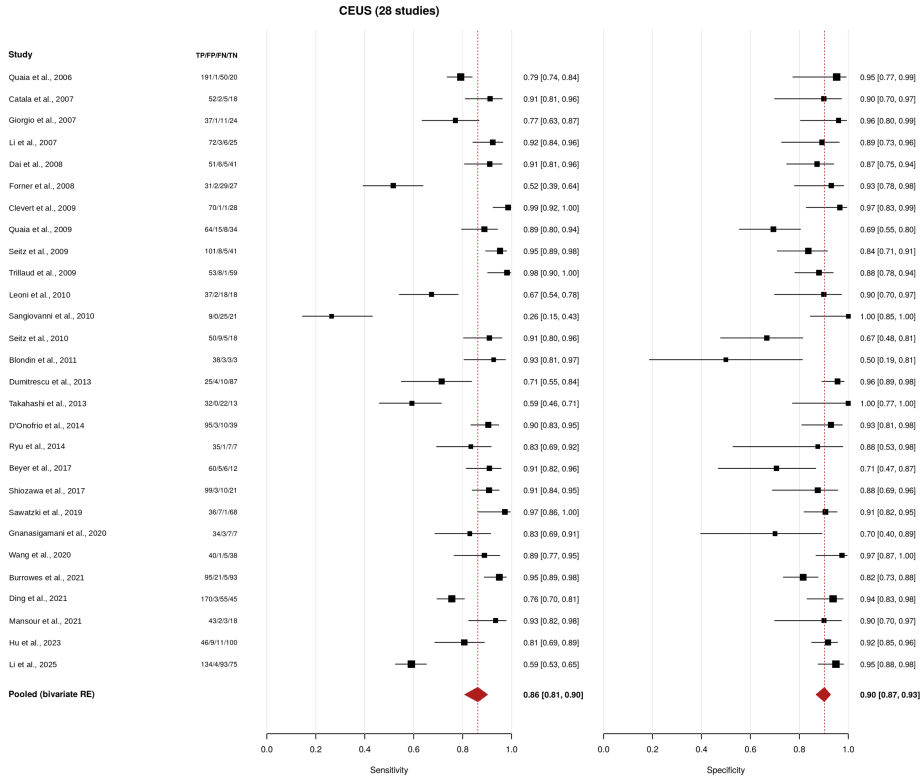


FIGURE 4: Forest plot of per-study sensitivity and specificity of CEUS (k = 28).

Included studies, ordered by publication year [26-53]. Squares are study estimates (size proportional to sample size) with 95% Wilson confidence intervals; the column beside each study name gives TP/FP/FN/TN. Diamonds and dashed vertical lines show the bivariate random-effects pooled estimates: sensitivity of 0.86 (0.81-0.90) and specificity of 0.90 (0.87-0.93).

CEUS, contrast-enhanced ultrasound; TP, true positive; FP, false positive; FN, false negative; TN, true negative; RE, random effects

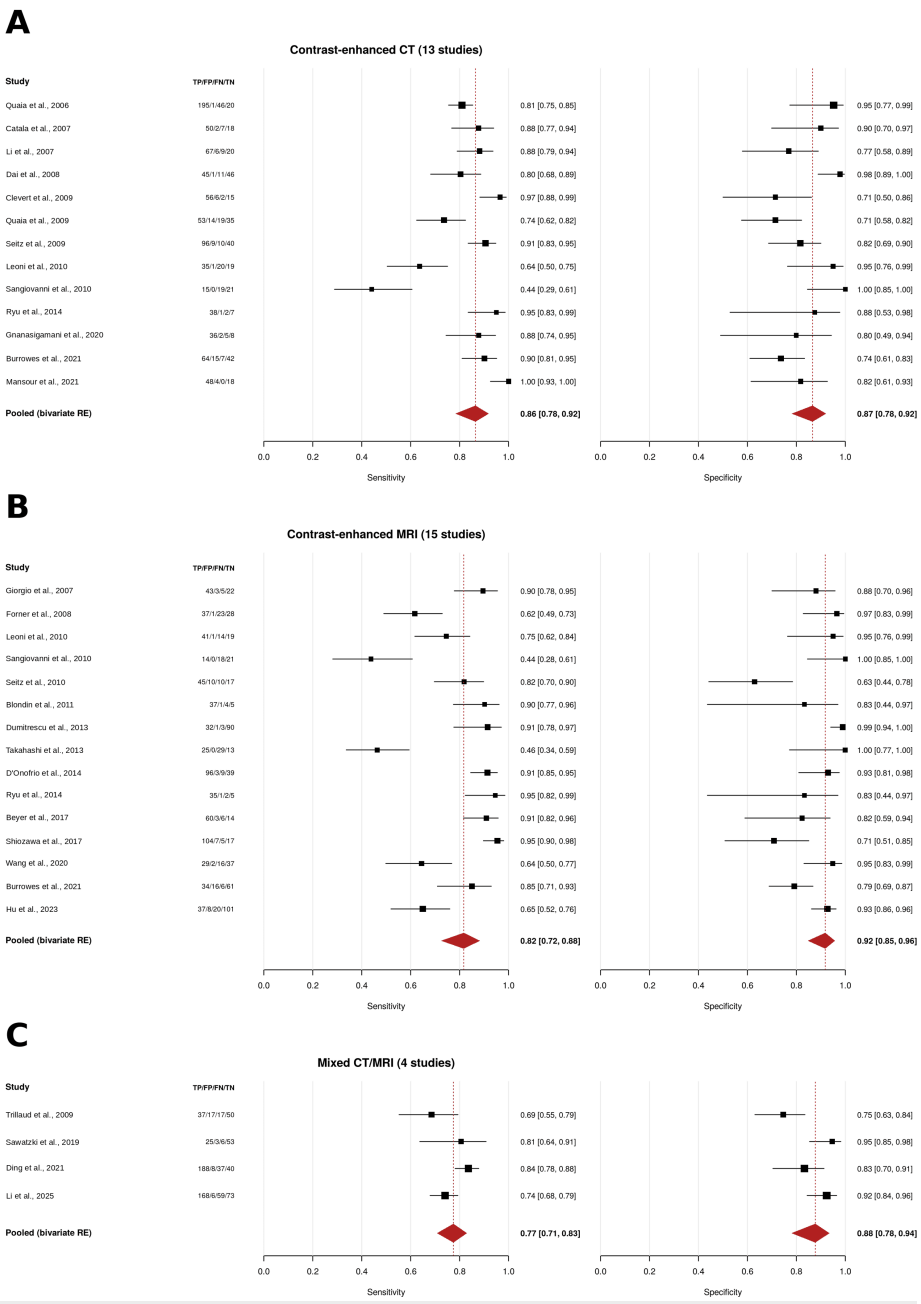


FIGURE 5: Forest plots of the per-study sensitivity and specificity of the comparator imaging tests.

(A) Contrast-enhanced CT, k = 13 [33,35-37,39,41,42,46,47,49-51,53]: pooled sensitivity of 0.86 (0.78-0.92) and specificity of 0.87 (0.78-0.92). (B) Contrast-enhanced MRI, k = 15 [27-32,34,38-43,47,48]: 0.82 (0.72-0.88) and 0.92 (0.85-0.96). (C) Mixed CT/MRI arms, k = 4 [26,44,45,52]: 0.77 (0.71-0.83) and 0.88 (0.78-0.94). Squares are study estimates with 95% Wilson confidence intervals; diamonds and dashed vertical lines show the bivariate random-effects pooled estimates.

CT, computed tomography; MRI, magnetic resonance imaging; TP, true positive; FP, false positive; FN, false negative; TN, true negative; RE, random effects

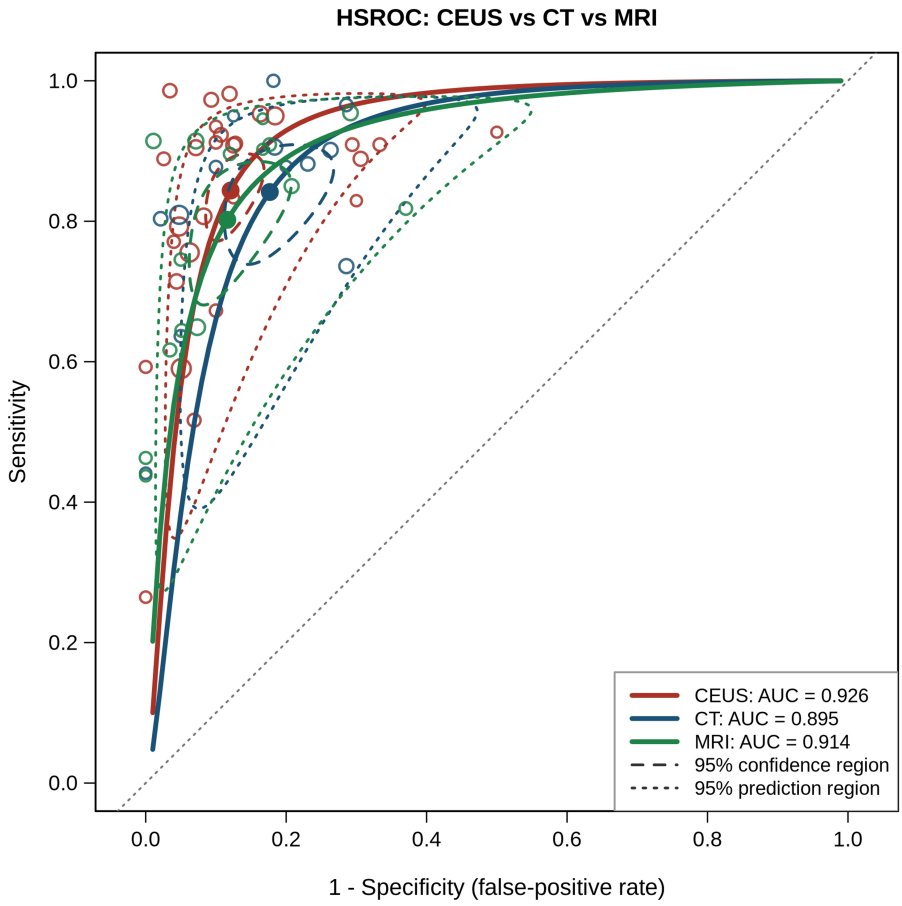


FIGURE 6: Hierarchical summary ROC curves for CEUS, CT, and MRI across all included arms.

Open circles are individual study arms in ROC space (CEUS [26-53]; CT [33,35-37,39,41,42,46,47,49-51,53]; MRI [27-32,34,38-43,47,48]), with circle size proportional to sample size. Solid points mark the summary operating points; dashed ellipses are 95% confidence regions and dotted ellipses 95% prediction regions. AUC: CEUS, 0.926; CT, 0.895; and MRI, 0.914. The dotted diagonal is the line of no discrimination.

ROC, receiver operating characteristic; AUC, area under the curve; CEUS, contrast-enhanced ultrasound; CT, computed tomography; MRI, magnetic resonance imaging; HSROC, hierarchical summary receiver operating characteristic

Head-to-Head Comparisons

Direct head-to-head comparisons were restricted to studies in which both tests were performed in the same patient cohorts (Figure *7A-7D*). In 13 studies comparing CEUS with CT [33,35-37,39,41,42,46,47,49-51,53], the sensitivity of CEUS was 88.0% (95% CI: 79.4%-93.4%) versus 86.5% (95% CI: 78.2%-91.9%) for CT (relative odds of sensitivity, CT versus CEUS, 0.90; 95% CI: 0.38-2.14; p = 0.812), and the specificity was 88.0% (95% CI: 81.7%-92.4%) versus 86.6% (95% CI: 78.0-92.2%) (relative odds, 0.78; 95% CI: 0.38-1.60; p = 0.504). In 15 studies comparing CEUS with MRI [27-32,34,38-43,47,48], the sensitivity was 81.6% (95% CI: 71.7%-88.7%) versus 81.7% (95% CI: 72.4%-88.3%) (relative odds, 1.01; 95% CI: 0.47-2.18; p = 0.977), and the specificity was 91.8% (95% CI: 85.7%-95.4%) versus 91.8% (95% CI: 84.7%-95.8%) (relative odds, 0.98; 95% CI: 0.39-2.44; p =0.962). In the four studies with mixed CT/MRI arms [26,44,45,52], the sensitivity was 89.5% (95% CI: 64.2%-97.6%) versus 77.5% (95% CI: 70.7%-83.0%) (relative odds, 0.50; 95% CI: 0.12-2.06; p = 0.328), and the specificity was 92.2% (95% CI: 87.2%-95.3%) versus 87.8% (95% CI: 78.0%-93.5%) (relative odds, 0.56; 95% CI: 0.24-1.30; p = 0.201). Across all 28 comparative studies, the sensitivity of CEUS was 86.2% versus 83.1% (95% CI: 77.7%-87.4%) for any CT/MRI arm (relative odds, 0.80; 95% CI: 0.47-1.36; p = 0.418), and the specificity was 90.2% versus 89.2% (95% CI: 84.6%-92.6%) (relative odds, 0.83; 95% CI: 0.49-1.42; p = 0.504). Joint likelihood-ratio tests showed no statistically significant difference in sensitivity and specificity between CEUS and any of the comparators (p = 0.214-0.999).

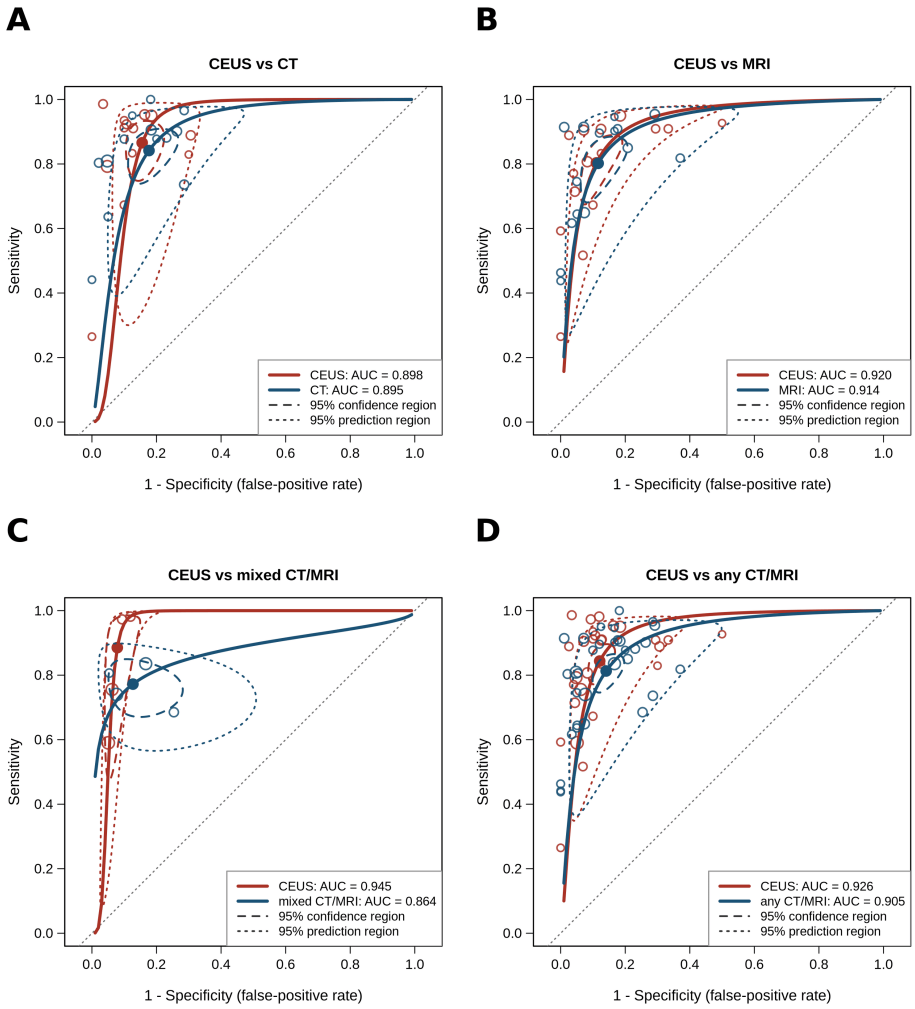


FIGURE 7: Head-to-head summary ROC curves: CEUS versus each comparator, restricted to studies reporting both tests.

(A) CEUS versus CT, 13 studies [33,35-37,39,41,42,46,47,49-51,53]: AUC of 0.898 versus 0.895. (B) CEUS versus MRI, 15 studies [27-32,34,38-43,47,48]: 0.920 versus 0.914. (C) CEUS versus mixed CT/MRI, four studies [26,44,45,52]: 0.945 versus 0.864. (D) CEUS versus any CT/MRI arm, 28 CEUS and 32 comparator arms [26-53]: 0.926 versus 0.905. Red, CEUS; blue, comparator. Dashed ellipses are 95% confidence regions and dotted ellipses 95% prediction regions.

ROC, receiver operating characteristic; AUC, area under the curve; CT, computed tomography; MRI, magnetic resonance imaging; CEUS, contrast-enhanced ultrasound

Heterogeneity, Subgroup Analyses, and Meta-Regression

Substantial between-study heterogeneity was observed, with an I^2 of 88.3% (95% CI: 84.3%-91.3%) for CEUS sensitivity and 57.0% (95% CI: 34.4%-71.8%) for CEUS specificity. A significant threshold effect was identified for CEUS ($\rho = 0.48$; $p = 0.009$) (Table *2*).

Test	Measure	k	I^2 (%)	I^2 95% CI	Cochran Q	df	p (Q)	τ^2	Threshold rho	Threshold p
CEUS	Sensitivity	28	88.3	84.3-91.3	231.6	27	2.11e-34	1	0.48	0.009
CEUS	Specificity	28	57	34.4-71.8	62.8	27	0.000113	0.373	0.48	0.009
CEUS	lnDOR	28	36.5	0-59.9	42.6	27	0.029	0.244	0.48	0.009
CT	Sensitivity	13	82.2	70.7-89.1	67.3	12	1.02e-09	0.765	0.52	0.071
CT	Specificity	13	38.8	0-68.2	19.6	12	0.0751	0.098	0.52	0.071
CT	lnDOR	13	47.9	1.1-72.6	23	12	0.0273	0.496	0.52	0.071
MRI	Sensitivity	15	87.1	80.4-91.5	108.7	14	1.01e-16	0.971	0.61	0.016
MRI	Specificity	15	64	37.4-79.3	38.9	14	0.000379	0.672	0.61	0.016
MRI	lnDOR	15	40.8	0-67.9	23.7	14	0.0503	0.456	0.61	0.016

TABLE 2: Between-study heterogeneity and threshold effect, by imaging test.

I^2, Q, and tau^2 are univariate random-effects statistics for each measure. Threshold rho is the Spearman correlation between logit sensitivity and logit(1 - specificity) across studies; a positive significant value indicates a threshold effect.

lnDOR, natural log of the diagnostic odds ratio; MRI, magnetic resonance imaging; CT, computed tomography; CEUS, contrast-enhanced ultrasound; CI, confidence interval; df, degrees of freedom

Bivariate meta-regression and subgroup analyses were performed to explore the sources of this heterogeneity. In univariable analyses, the target condition was significantly associated with CEUS sensitivity: studies focusing specifically on HCC [26,27,29-31,34,36,41,42,52] reported a lower pooled sensitivity (68.7%, 95% CI: 58.9%-77.2%) than those assessing overall malignancy [28,32,33,35,37,39,40,43-48,50,51,53] (92.4%, 95% CI: 89.2%-94.8%) ($p_{sens} < 0.001$). CEUS sensitivity was also higher in non-cirrhotic/mixed cohorts [27,28,32,33,35,37-39,44-50,53] (91.6%) than in strictly cirrhotic/at-risk cohorts [26,29-31,34,36,40-43,51,52] (74.6%) ($p_{sens} < 0.001$), and studies restricted to small nodules (≤20-30 mm) [29,30,34,36,41,42] were associated with a lower sensitivity (64.6%) but higher specificity (94.8%) than studies with unrestricted lesion sizes (sensitivity, 89.6%; specificity, 88.5%). Because all six small-nodule studies evaluated HCC in cirrhotic cohorts, these covariates overlapped substantially. In a multivariable bivariate meta-regression including the three covariates simultaneously, only the target condition remained independently associated with CEUS accuracy (HCC versus other target conditions: odds ratio for sensitivity, 0.31; 95% CI: 0.13-0.78; p = 0.018; odds ratio for specificity, 4.32; 95% CI: 1.80-10.41; p = 0.002), whereas liver background (joint p = 0.27) and lesion-size restriction (joint p = 0.62) were not.

Lesion-Specific Accuracy and Size Strata

Lesion-specific analysis (Table *3*) demonstrated that for HCC characterization (k = 12) [26,27,29-34,36,41,42,52], CEUS achieved a sensitivity of 71.6% and a specificity of 94.6%, directly comparable to the CT/MRI arms (sensitivity, 71.0%; specificity, 95.9%). For the characterization of liver metastases (k = 4) [32,33,38,49], CEUS showed numerically higher sensitivity (86.2% versus 81.3%) and specificity (82.0% versus 77.6%) than the CT/MRI arms, with overlapping confidence intervals (Table *3*); these studies assessed the characterization of lesions identified on imaging rather than the whole-liver detection of metastases.

Analysis	k	Diseased (n)	Non-diseased (n)	Sensitivity, % (95% CI)	Specificity, % (95% CI)	LR+ (95% CI)	LR- (95% CI)	DOR (95% CI)	τ^2 logit sensitivity	τ^2 logit specificity	Rho
HCC-CEUS	12	904	584	71.6 (60.6-80.5)	94.6 (90.8-96.8)	13.15 (7.94-21.76)	0.30 (0.21-0.42)	43.8 (23.9-80.1)	0.646	0.416	-0.6
HCC-CT/MRI arms	14	991	625	71.0 (62.4-78.3)	95.9 (91.3-98.1)	17.15 (8.48-34.69)	0.30 (0.23-0.39)	56.6 (29.1-110.1)	0.44	1.125	-0.83
Metastasis-CEUS	4	419	213	86.2 (77.9-91.7)	82.0 (76.2-86.7)	4.80 (3.53-6.51)	0.17 (0.10-0.28)	28.6 (14.2-57.3)	0.211	0.002	1
Metastasis-CT/MRI arms	4	419	213	81.3 (63.7-91.5)	77.6 (71.4-82.8)	3.63 (2.73-4.82)	0.24 (0.12-0.50)	15.1 (6.0-37.9)	0.741	0.003	-1
Hemangioma-CEUS (descriptive)	3	25	260	72.0 (52.4-85.7)	93.5 (89.8-95.9)	NA	NA	NA	NA	NA	NA
Hemangioma-CT/MRI arms (descriptive)	3	26	261	76.9 (57.9-89.0)	93.5 (89.8-95.9)	NA	NA	NA	NA	NA	NA
FNH-CEUS (descriptive)	2	37	166	67.6 (51.5-80.4)	97.6 (94.0-99.1)	NA	NA	NA	NA	NA	NA
FNH-CT/MRI arms (descriptive)	2	38	167	71.1 (55.2-83.0)	98.8 (95.7-99.7)	NA	NA	NA	NA	NA	NA

TABLE 3: Lesion-specific accuracy of CEUS and CT/MRI arms for HCC, metastasis, hemangioma, and focal nodular hyperplasia.

HCC and metastasis rows are bivariate random-effects estimates. Hemangioma and FNH rows are descriptive: counts summed across studies with Wilson intervals because too few studies were available for a model.

NA, not estimated; FNH, focal nodular hyperplasia; HCC, hepatocellular carcinoma; CT, computed tomography; MRI, magnetic resonance imaging; CEUS, contrast-enhanced ultrasound; CI, confidence interval; DOR, diagnostic odds ratio; LR, likelihood ratio

Data for nodules of ⩽20 mm were obtained from the three studies restricted to nodules of ⩽20 mm [34,36,41] and from the size strata explicitly reported in two studies without this restriction: the <20 mm stratum of [26] and the 10-19 mm stratum of [42]; only strata reported by the primary studies were used, and the study-level counts are listed in the Appendices. In this analysis (Table *4*), comprising five CEUS arms (220 diseased and 141 non-diseased lesions) and seven CT/MRI arms (279 diseased and 178 non-diseased lesions), CEUS maintained high specificity (96.0%) but demonstrated diminished sensitivity (57.9%), mirroring the performance of CT/MRI in this challenging size stratum (sensitivity, 62.9%; specificity, 97.3%).

Analysis	k	Diseased (n)	Non-diseased (n)	Sensitivity, % (95% CI)	Specificity, % (95% CI)	LR+ (95% CI)	LR- (95% CI)	DOR (95% CI)	τ^2 logit sensitivity	τ^2 logit specificity	Rho
≤20 mm-CEUS	5	220	141	57.9 (34.9-77.9)	96.0 (90.0-98.5)	14.47 (6.73-31.09)	0.44 (0.26-0.74)	33.0 (14.1-77.0)	1.033	0.538	-1
≤20 mm-CT/MRI arms	7	279	178	62.9 (52.5-72.3)	97.3 (93.6-98.9)	23.47 (9.79-56.29)	0.38 (0.29-0.50)	61.6 (23.8-159.3)	0.22	0.038	-1

TABLE 4: Pooled accuracy for nodules of ≤20 mm: CEUS versus CT/MRI arms.

Rho at the boundary (-1) reflects the small number of arms.

CT, computed tomography; MRI, magnetic resonance imaging; CEUS, contrast-enhanced ultrasound; CI, confidence interval; DOR, diagnostic odds ratio; LR, likelihood ratio

Sensitivity Analyses and Publication Bias

The robustness of the pooled estimates was examined in sensitivity analyses. Five studies contained internal inconsistencies: In Dumitrescu et al.'s study [27], the cross-tabulated data were compatible with 35 HCC and 91 non-HCC lesions, whereas the text reported 76 HCCs; in Clevert et al.'s study [35], the number of true positive results (70) exceeded the stated number of malignant lesions (59); in Gnanasigamani et al.'s study [46], the definition of a positive test was not specified; in Ryu et al.'s study [47], the reported sensitivity and specificity implied 42 malignant and eight benign lesions, whereas the tabulated data listed 44 and six; and in Mansour et al.'s study [53], the reported accuracy measures could not be reproduced from the published counts. Excluding these five studies yielded a pooled sensitivity of 85.5% (95% CI: 78.9%-90.3%) and specificity of 90.1% (95% CI: 85.9%-93.2%), compared with 86.2% and 90.2% in the full analysis. Restricting the analysis to studies with blinded index test reading [26,29-31,34-37,39-43,49-52] gave a sensitivity of 82.0% (95% CI: 72.4%-88.8%) and a specificity of 91.9% (95% CI: 87.2%-95.0%); to studies with a histological reference standard [29-34,36,37,41,43,46,51,52], 82.6% (95% CI: 71.7%-89.9%) and 90.2% (95% CI: 81.0%-95.2%); to per-lesion analyses, 84.2% (95% CI: 77.0%-89.4%) and 90.5% (95% CI: 85.6%-93.8%); and excluding Seitz et al.'s study [32] because of possible cohort overlap with Seitz et al.'s study [33], 86.0% (95% CI: 80.1%-90.4%) and 90.7% (95% CI: 87.4%-93.2%). The unit of analysis (per-lesion versus per-patient) was not significantly associated with sensitivity (p = 0.16) or specificity (p = 0.96). Leave-one-out influence analyses confirmed that no single study disproportionately affected the pooled sensitivity (range: 85.3%-87.2%) or specificity (range: 89.6%-90.8%) (Figure *8*) [26-53].

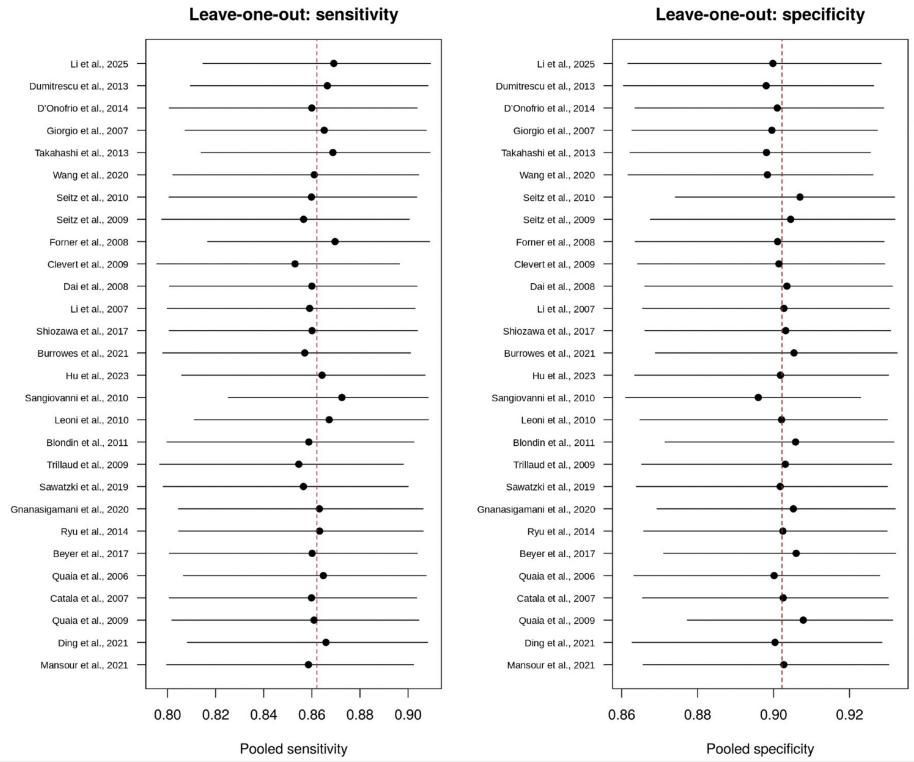


FIGURE 8: Leave-one-out influence analysis for the pooled accuracy of CEUS.

Left, pooled sensitivity; right, pooled specificity. Each point is the bivariate estimate (95% CI) after omitting the named study [26-53]; the dashed vertical line is the full-data estimate.

CEUS, contrast-enhanced ultrasound; CI, confidence interval

The visual inspection of contour-enhanced funnel plots and Deeks' funnel plot asymmetry test did not detect significant asymmetry for either CEUS (p = 0.555) or the CT/MRI comparator arms (p = 0.330) (Figure *9A*, *9B*) [23]. Because Deeks' test has limited statistical power with the number of studies available, these findings do not exclude publication bias or small-study effects and should be interpreted with caution.

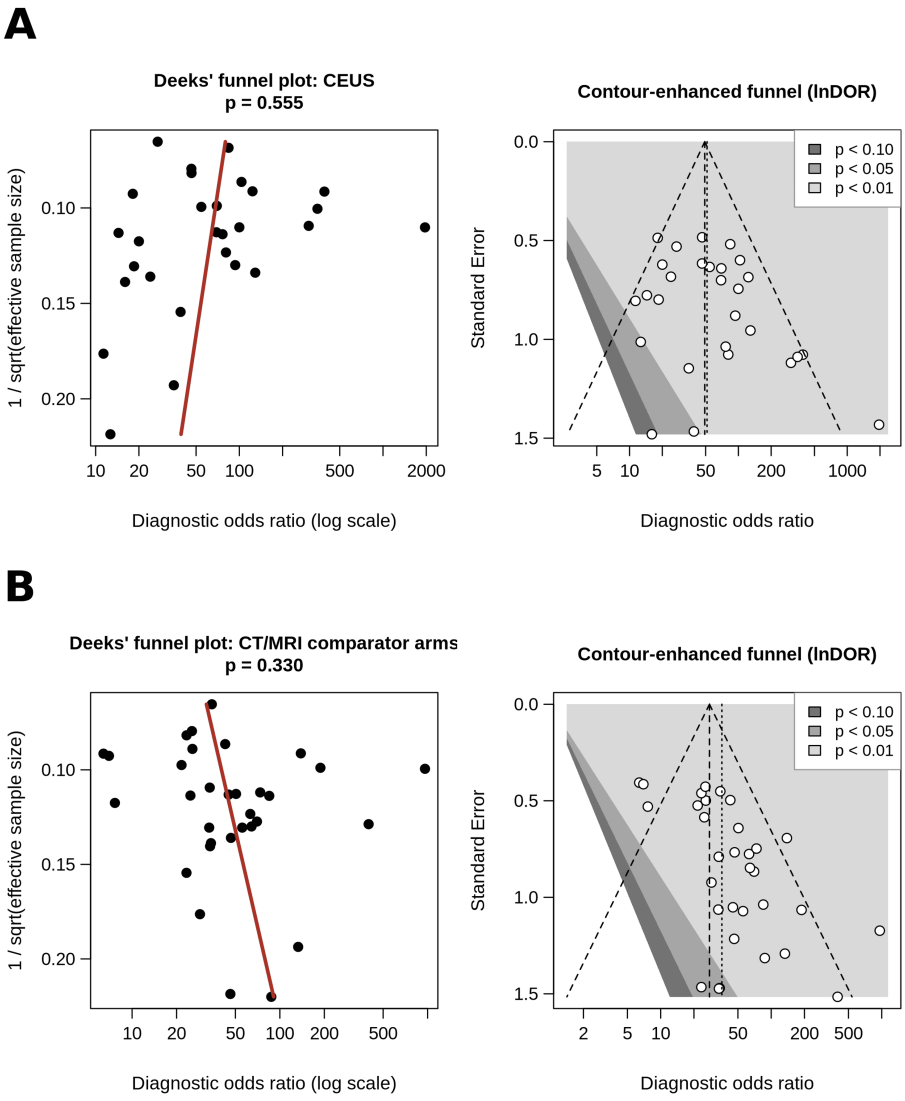


FIGURE 9: Assessment of publication bias.

(A) CEUS, k = 28 [26-53]; Deeks' test; p = 0.555. (B) CT/MRI comparator arms, k = 32 [26-53]; p = 0.330. In each panel, the left plot is Deeks' funnel plot of the diagnostic odds ratio (log scale) against 1/sqrt(effective sample size) with the fitted regression line [23]. The right plot is a contour-enhanced funnel of lnDOR against its standard error, shaded by significance level (p < 0.10, < 0.05, and < 0.01).

lnDOR, natural logarithm of the diagnostic odds ratio; CEUS, contrast-enhanced ultrasound; CT, computed tomography; MRI, magnetic resonance imaging

Clinical Utility and Certainty of Evidence

The clinical utility of CEUS in practice was modelled using Fagan's nomograms (Figure *10*) [24]. Assuming a median pre-test probability (the prevalence of the target condition) of 70% across the CEUS arms, a positive CEUS finding generated a post-test probability (positive predictive value, PPV) of 95.4%, whereas a negative finding reduced the probability of the target condition to 26.3%, corresponding to a negative predictive value (NPV) of 73.7% [26-53]. These values were comparable to those of CT (PPV, 93.8%; NPV, 73.3%) and MRI (PPV, 95.9%; NPV, 68.2%) at the same pre-test probability. Because a prevalence of 70% reflects the referral populations of the included studies rather than routinely encountered incidental lesions, post-test probabilities were also calculated at lower pre-test probabilities: At 10%, 25%, and 50%, the PPV of CEUS was 49.5%, 74.6%, and 89.8%, and its NPV was 98.3%, 95.1%, and 86.7%, respectively (see Appendices).

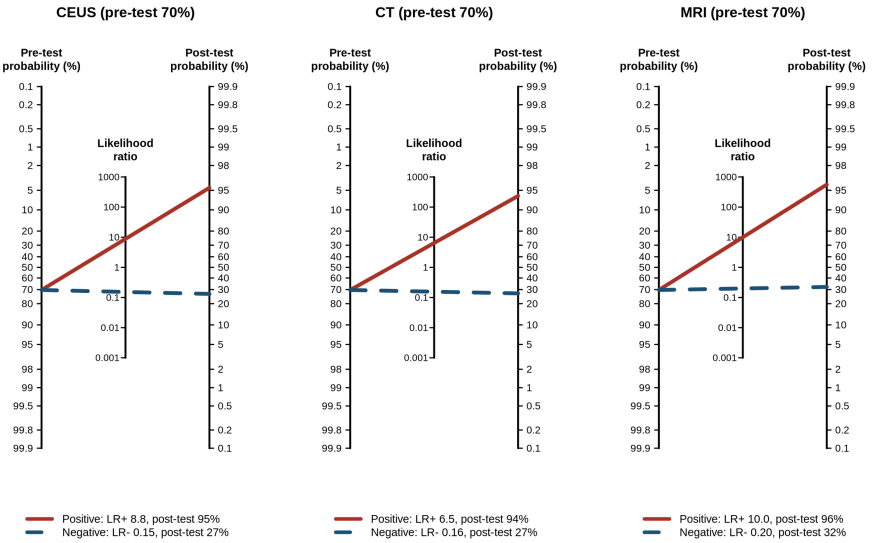


FIGURE 10: Fagan's nomograms for CEUS, CT, and MRI at a pre-test probability of 70%.

Nomograms after Fagan's study [24]. The pre-test probability (70.3%) is the median prevalence across the CEUS arms [26-53]. Solid red line, positive result; dashed blue line, negative result. Post-test probability after a positive/negative result: CEUS, 95%/27%; CT, 94%/27%; MRI, 96%/32%.

LR, likelihood ratio; CEUS, contrast-enhanced ultrasound; CT, computed tomography; MRI, magnetic resonance imaging

Utilizing the GRADE framework (Table *5*), the overall certainty of evidence was adjudicated as low [25]. While evidence was not downgraded for imprecision, indirectness, or publication bias, it was downgraded due to serious risk of bias (methodological limitations across primary studies) and serious inconsistency (unexplained residual heterogeneity, $I^2 > 75\%$).

Test	Risk of bias	Indirectness	Inconsistency	Imprecision	Publication bias	Suggested certainty
CEUS	Serious (-1): >50% of studies with high RoB in ≥1 domain	Not serious (direct head-to-head populations); consider -1 for mixed target conditions	Serious (-1): $I^2 > 75\%$, partly explained by subgroups	Not serious	Undetected	Low
CT	Serious (-1)	Not serious (direct head-to-head populations); consider -1 for mixed target conditions	Serious (-1): $I^2 > 75\%$, partly explained by subgroups	Not serious	Undetected	Low
MRI	serious (-1): >50% of studies with high RoB in ≥1 domain	Not serious (direct head-to-head populations); consider -1 for mixed target conditions	Serious (-1): $I^2 > 75\%$, partly explained by subgroups	Not serious	Undetected	Low

TABLE 5: GRADE certainty of evidence: suggested domain judgements, by imaging test.

RoB, risk of bias; GRADE, Grading of Recommendations Assessment, Development, and Evaluation; CT, computed tomography; MRI, magnetic resonance imaging; CEUS, contrast-enhanced ultrasound

Discussion

This systematic review and meta-analysis provides an updated evaluation of the diagnostic accuracy of CEUS compared with multiphasic CT and MRI for the characterization of FLLs. Synthesizing data from 28 studies comprising 60 study arms, our findings demonstrate that CEUS exhibits high overall diagnostic performance, with a pooled sensitivity of 86.2% and specificity of 90.2%, alongside an AUC of 0.926 [26-53]. In direct head-to-head comparisons within the same patient cohorts, there was no statistically significant difference

in sensitivity or specificity between CEUS and CECT or CEMRI, supporting its role as a reliable complementary imaging modality in hepatology practice.

Our results align with and expand upon those of previous meta-analyses. Westwood et al. [3] and Ren et al. [8] previously reported comparable diagnostic accuracies between CEUS, CT, and MRI, although their analyses were limited by the availability of contemporary studies utilizing standardized reporting systems. This analysis integrates more recent literature, including studies applying CEUS LI-RADS [26,31,40,52], which has standardized interpretation and enhanced the clinical utility of CEUS, particularly for HCC [26,52].

However, the diagnostic performance of CEUS was not uniform across all clinical scenarios, as evidenced by substantial inter-study heterogeneity (I^2 = 88.3% for sensitivity). In univariable bivariate meta-regression, the target condition and the underlying liver parenchyma were associated with this variance; after mutual adjustment, only the target condition remained independently associated with accuracy, because all small-nodule studies evaluated HCC in cirrhotic cohorts and these covariates therefore overlapped substantially. CEUS demonstrated a lower pooled sensitivity (68.7%) for the specific diagnosis of HCC compared to its sensitivity for overall malignancy (92.4%), reflecting the stringent diagnostic criteria required for HCC (e.g., arterial-phase hyperenhancement, followed by late and mild washout), which, while ensuring high specificity (94.6%), compromises sensitivity [4,10,11]. Furthermore, the performance of CEUS was lower in cirrhotic/at-risk livers (sensitivity: 74.6%) compared to non-cirrhotic backgrounds (sensitivity: 91.6%). The coarse, nodular echotexture of cirrhotic livers, combined with the presence of regenerative and dysplastic nodules that can mimic malignancy, poses challenges for ultrasound-based characterization, even with contrast enhancement [2,12].

Lesion size emerged as another critical determinant of diagnostic accuracy. In subgroup analyses, small nodules (≤20-30 mm) were associated with reduced sensitivity (64.6%) but maintained high specificity (94.8%). This observation underscores the technical limitations of CEUS and, indeed, cross-sectional imaging in characterizing subcentimeter or small lesions, where the classic vascular hallmarks of malignancy may be less pronounced or technically difficult to resolve [6,13]. Despite this, CEUS performed comparably with CT and MRI within this challenging size stratum, highlighting its utility as a complementary tool when cross-sectional imaging yields indeterminate results.

For the characterization of liver metastases, CEUS showed numerically higher sensitivity (86.2%) than CT/MRI (81.3%), with overlapping confidence intervals [32,33,38,49]. The real-time nature of CEUS, which allows for the continuous observation of the entire vascular phase, is advantageous in capturing the rapid, transient arterial enhancement and rapid washout characteristic of many metastatic lesions, which might be missed between the discrete acquisition phases of CT or MRI [7,9]. This observation applies to the characterization of lesions already identified; for whole-liver detection and staging of metastatic disease, the limited field of view of CEUS and the dynamic assessment of only one or a few lesions per contrast injection favor CT and MRI.

The clinical implications of these findings are substantial. Modelled via Fagan's nomograms, a positive CEUS finding increases the post-test probability of malignancy, providing diagnostic confidence comparable with that of CT and MRI. Given its advantages, including the absence of ionizing radiation, the lack of nephrotoxicity, lower cost, and bedside applicability, CEUS is a valuable problem-solving tool following an indeterminate unenhanced ultrasound examination and a complementary option to CT or MRI in selected patients, which is particularly relevant for patients with renal impairment or contrast allergies or those requiring repeated imaging for surveillance [1,5,8].

This meta-analysis is strengthened by its adherence to PRISMA-DTA guidelines, comprehensive search strategy, and the use of robust hierarchical bivariate models. Furthermore, the inclusion of direct head-to-head comparisons minimizes confounding by patient cohort differences. However, several limitations must be acknowledged. First, the overall certainty of evidence was graded as low according to the GRADE framework, driven by the serious risk of bias identified in the patient selection and reference standard domains of several primary studies, as well as the substantial, partially unexplained heterogeneity. Second, the reliance on a composite reference standard (histopathology and/or imaging follow-up) in many studies introduces the potential for differential verification bias [26-28,35,38-40,42,44,45,47-50,53]. Finally, while we attempted to explore the impact of specific contrast agents (e.g., sulfur hexafluoride versus perfluorobutane), the limited number of studies utilizing agents other than SonoVue precluded definitive conclusions regarding agent-specific performance [30,38-40].

Conclusions

CEUS showed high diagnostic accuracy for the characterization of focal liver lesions, with no statistically significant difference in sensitivity or specificity compared with CECT and CEMRI in head-to-head comparisons. However, given the low certainty of the evidence, the substantial heterogeneity, and the lower sensitivity for HCC-specific diagnosis and for small nodules, CEUS is best regarded as a complementary, context-dependent modality rather than a replacement for cross-sectional imaging, particularly for problem-solving in lesions that remain indeterminate on unenhanced ultrasound or CT/MRI and for patients

in whom CT or MRI contrast agents are contraindicated. Future research should prioritize large, prospective, multicenter studies with standardized LI-RADS reporting and strict histological reference standards to solidify the evidence base and elevate the certainty of these findings.

Appendices

Table *6* shows the complete database-specific search strategies.

Database/source	Search strategy
PubMed/MEDLINE	#1 ("Ultrasonography"[Mesh] AND ("Contrast Media"[Mesh] OR "Microbubbles"[Mesh])) OR "contrast-enhanced ultrasound"[tiab] OR "contrast enhanced ultrasound"[tiab] OR "contrast-enhanced ultrasonography"[tiab] OR "contrast-enhanced sonography"[tiab] OR CEUS[tiab] OR SonoVue[tiab] OR Lumason[tiab] OR Sonazoid[tiab] OR Definity[tiab] OR perflubutane[tiab] OR perflutren[tiab] OR "sulfur hexafluoride"[tiab] OR "sulphur hexafluoride"[tiab] OR microbubble*[tiab]; #2 "Tomography, X-Ray Computed"[Mesh] OR "Magnetic Resonance Imaging"[Mesh] OR "computed tomography"[tiab] OR CT[tiab] OR CECT[tiab] OR MDCT[tiab] OR "magnetic resonance"[tiab] OR MRI[tiab] OR CEMRI[tiab] OR gadoxetic[tiab] OR "Gd-EOB-DTPA"[tiab]; #3 "Liver Neoplasms"[Mesh] OR "Carcinoma, Hepatocellular"[Mesh] OR "Focal Nodular Hyperplasia"[Mesh] OR "Adenoma, Liver Cell"[Mesh] OR "Hemangioma"[Mesh] OR ((focal[tiab] OR solid[tiab] OR incidental[tiab]) AND (liver[tiab] OR hepatic[tiab]) AND (lesion*[tiab] OR mass*[tiab] OR nodule*[tiab] OR tumor*[tiab] OR tumour*[tiab])) OR "hepatocellular carcinoma"[tiab] OR HCC[tiab] OR "liver metastas*"[tiab] OR "hepatic metastas*"[tiab]; #4 #1 AND #2 AND #3 NOT ("Animals"[Mesh] NOT "Humans"[Mesh])
Embase (Embase.com)	#1 "contrast enhanced ultrasound"/exp OR "microbubble"/exp OR "sulfur hexafluoride"/exp OR "perflubutane"/exp OR "perflutren"/exp OR ("contrast enhanced ultrasound" OR "contrast-enhanced ultrasonography" OR "contrast-enhanced sonography" OR ceus OR sonovue OR lumason OR sonazoid OR definity OR microbubble*):ti,ab,kw; #2 "computer assisted tomography"/exp OR "nuclear magnetic resonance imaging"/exp OR ("computed tomography" OR ct OR cect OR mdct OR "magnetic resonance" OR mri OR cemri OR gadoxetic):ti,ab,kw; #3 "liver tumor"/exp OR "liver cell carcinoma"/exp OR "liver metastasis"/exp OR "focal nodular hyperplasia"/exp OR "liver hemangioma"/exp OR "liver cell adenoma"/exp OR ((liver OR hepatic) NEAR/3 (lesion* OR nodule* OR mass* OR tumor* OR tumour* OR metastas*)):ti,ab,kw OR ("hepatocellular carcinoma" OR hcc):ti,ab,kw; #4 #1 AND #2 AND #3 NOT ("animal"/exp NOT "human"/exp)
Cochrane CENTRAL	#1 MeSH descriptor: [Contrast Media] explode all trees OR MeSH descriptor: [Microbubbles] explode all trees OR ("contrast-enhanced ultrasound" OR "contrast enhanced ultrasonography" OR "contrast-enhanced sonography" OR CEUS OR SonoVue OR Lumason OR Sonazoid OR Definity OR microbubble*):ti,ab,kw; #2 MeSH descriptor: [Tomography, X-Ray Computed] explode all trees OR MeSH descriptor: [Magnetic Resonance Imaging] explode all trees OR ("computed tomography" OR CT OR CECT OR "magnetic resonance" OR MRI OR CEMRI):ti,ab,kw; #3 MeSH descriptor: [Liver Neoplasms] explode all trees OR ((liver OR hepatic) NEAR/3 (lesion* OR nodule* OR mass* OR tumor* OR tumour* OR metastas*)):ti,ab,kw OR ("hepatocellular carcinoma" OR HCC):ti,ab,kw; #4 #1 AND #2 AND #3
Scopus	TITLE-ABS-KEY(("contrast-enhanced ultrasound" OR "contrast enhanced ultrasonography" OR "contrast-enhanced sonography" OR ceus OR sonovue OR lumason OR sonazoid OR definity OR microbubble*) AND ("computed tomography" OR ct OR cect OR mdct OR "magnetic resonance" OR mri OR cemri) AND (((liver OR hepatic) W/3 (lesion* OR nodule* OR mass* OR tumor* OR tumour* OR metastas*)) OR "hepatocellular carcinoma" OR hcc))
Web of Science Core Collection	TS=(("contrast-enhanced ultrasound" OR "contrast enhanced ultrasonography" OR "contrast-enhanced sonography" OR CEUS OR SonoVue OR Lumason OR Sonazoid OR Definity OR microbubble*) AND ("computed tomography" OR CT OR CECT OR MDCT OR "magnetic resonance" OR MRI OR CEMRI) AND (((liver OR hepatic) NEAR/3 (lesion* OR nodule* OR mass* OR tumor* OR tumour* OR metastas*)) OR "hepatocellular carcinoma" OR HCC))
ClinicalTrials.gov	Condition/disease: liver lesion OR liver neoplasm OR hepatocellular carcinoma OR liver metastases; Intervention/treatment: contrast-enhanced ultrasound OR CEUS OR SonoVue OR Sonazoid OR Definity
WHO ICTRP	(contrast-enhanced ultrasound OR CEUS OR SonoVue OR Sonazoid OR Definity) AND (liver OR hepatic OR hepatocellular)

TABLE 6: Database-specific electronic search strategies.

Search strings are shown as entered in each database, combining controlled vocabulary (MeSH/Emtree) with free-text terms, Boolean operators, and truncation. No language, publication-date, or study-design filters were applied.

MeSH, Medical Subject Headings; tiab, title/abstract; ti,ab,kw, title/abstract/keywords; TS, topic; CEUS, contrast-enhanced ultrasound; CT, computed tomography; MRI, magnetic resonance imaging; HCC, hepatocellular carcinoma; WHO ICTRP, World Health Organization International Clinical Trials Registry Platform; CEMRI, contrast-enhanced magnetic resonance imaging; MEDLINE, Medical Literature Analysis and Retrieval System Online; CENTRAL, Cochrane Central Register of Controlled Trials; CECT, contrast-enhanced computed tomography; MDCT, multidetector computed tomography

Table 7 shows the extracted 2 × 2 tables for every study and imaging modality.

Study and reference	Test	Positive test definition	Analysis set	TP	FP	FN	TN
Li et al., 2025 [26]	CEUS	CEUS LI-RADS LR-5 (SonoVue)	Primary analysis	134	4	93	75

Li et al., 2025 [26]	CT/MRI (mixed)	CT/MRI LI-RADS LR-5	Primary analysis	168	6	59	73
Dumitrescu et al., 2013 [27]	CEUS	Typical HCC pattern	Primary analysis	25	4	10	87
Dumitrescu et al., 2013 [27]	MRI	Gd-DTPA dynamic MRI	Primary analysis	32	1	3	90
D'Onofrio et al., 2014 [28]	CEUS	Late-phase hypoenhancement	Primary analysis	95	3	10	39
D'Onofrio et al., 2014 [28]	MRI	Gd-BOPTA hepatobiliary phase	Primary analysis	96	3	9	39
Giorgio et al., 2007 [29]	CEUS	Arterial hypervascularity	Primary analysis	37	1	11	24
Giorgio et al., 2007 [29]	MRI	Dynamic Gd MRI typical pattern	Primary analysis	43	3	5	22
Takahashi et al., 2013 [30]	CEUS	Arterial-phase hyperenhancement	Primary analysis	32	0	22	13
Takahashi et al., 2013 [30]	MRI	EOB-MRI arterial-phase hyperenhancement	Primary analysis	25	0	29	13
Wang et al., 2020 [31]	CEUS	LR-5/LR-TIV reviewer 1	Primary analysis	40	1	5	38
Wang et al., 2020 [31]	MRI	LR-5/LR-TIV reviewer 1 (Gd-DTPA)	Primary analysis	29	2	16	37
Seitz et al., 2010 [32]	CEUS	Malignant versus benign (histology subgroup B)	Primary analysis	50	9	5	18
Seitz et al., 2010 [32]	MRI	malignant versus benign (histology subgroup B)	Primary analysis	45	10	10	17
Seitz et al., 2009 [33]	CEUS	malignant versus benign (histology subgroup B)	Primary analysis	101	8	5	41
Seitz et al., 2009 [33]	CT	Spiral CT	Primary analysis	96	9	10	40
Forner et al., 2008 [34]	CEUS	Arterial uptake + washout	Primary analysis	31	2	29	27
Forner et al., 2008 [34]	MRI	Dynamic MRI arterial uptake + washout	Primary analysis	37	1	23	28
Clevert et al., 2009 [35]	CEUS	Quantitative CHI	Primary analysis	70	1	1	28
Clevert et al., 2009 [35]	CT	Biphasic MSCT	Primary analysis	56	6	2	15
Dai et al., 2008 [36]	CEUS	Arterial enhancement + washout	Primary analysis	51	6	5	41
Dai et al., 2008 [36]	CT	Helical CECT	Primary analysis	45	1	11	46
Li et al., 2007 [37]	CEUS	Malignant versus benign	Primary analysis	72	3	6	25
Li et al., 2007 [37]	CT	Helical CECT	Primary analysis	67	6	9	20
Shiozawa et al., 2017 [38]	CEUS	Confidence ≥4 for metastasis	Primary analysis	99	3	10	21
Shiozawa et al., 2017 [38]	MRI	EOB-MRI confidence ≥4	Primary analysis	104	7	5	17
Burrowes et al., 2021 [39]	CEUS	Malignant versus benign (all 214)	Primary analysis	95	21	5	93
Burrowes et al., 2021 [39]	CT	CT subset (n = 128)	Primary analysis	64	15	7	42
Burrowes et al., 2021 [39]	MRI	MRI subset (n = 117)	Primary analysis	34	16	6	61
Hu et al., 2023 [40]	CEUS	LR-5/LR-M = malignant	Primary analysis	46	9	11	100
Hu et al., 2023 [40]	MRI	LR-5/LR-M = malignant	Primary analysis	37	8	20	101
Sangiovanni et al., 2010 [41]	CEUS	Typical vascular pattern 1-2 cm	Primary analysis	9	0	25	21
Sangiovanni et al., 2010 [41]	CT	Typical vascular pattern 1-2 cm	Primary analysis	15	0	19	21
Sangiovanni et al., 2010 [41]	MRI	Typical vascular pattern 1-2 cm	Primary analysis	14	0	18	21
Leoni et al., 2010 [42]	CEUS	AASLD criteria overall	Primary analysis	37	2	18	18
Leoni et al., 2010 [42]	CT	AASLD criteria overall	Primary analysis	35	1	20	19
Leoni et al., 2010 [42]	MRI	AASLD criteria overall (gad-MR)	Primary analysis	41	1	14	19
Blondin et al., 2011 [43]	CEUS	Malignant versus benign	Primary analysis	38	3	3	3

Blondin et al., 2011 [43]	MRI	EOB-MRI	Primary analysis	37	1	4	5
Trillaud et al., 2009 [44]	CEUS	Malignant versus benign	Primary analysis	53	8	1	59
Trillaud et al., 2009 [44]	CT/MRI (mixed)	CT and/or MRI	Primary analysis	37	17	17	50
Sawatzki et al., 2019 [45]	CEUS	Washout = malignant	Primary analysis	36	7	1	68
Sawatzki et al., 2019 [45]	CT/MRI (mixed)	CT or MRI (n = 87)	Primary analysis	25	3	6	53
Gnanasigamani et al., 2020 [46]	CEUS	Positive versus histopathology	Primary analysis	34	3	7	7
Gnanasigamani et al., 2020 [46]	CT	CECT	Primary analysis	36	2	5	8
Ryu et al., 2014 [47]	CEUS	Malignant versus benign	Primary analysis	35	1	7	7
Ryu et al., 2014 [47]	CT	CT (n = 48)	Primary analysis	38	1	2	7
Ryu et al., 2014 [47]	MRI	MRI (n = 43)	Primary analysis	35	1	2	5
Beyer et al., 2017 [48]	CEUS	Malignant versus benign	Primary analysis	60	5	6	12
Beyer et al., 2017 [48]	MRI	Liver-specific MRI	Primary analysis	60	3	6	14
Quaia et al., 2006 [49]	CEUS	Metastasis per lesion (SonoVue subset)	Primary analysis	191	1	50	20
Quaia et al., 2006 [49]	CT	CECT (SonoVue subset)	Primary analysis	195	1	46	20
Catala et al., 2007 [50]	CEUS	Malignant versus benign	Primary analysis	52	2	5	18
Catala et al., 2007 [50]	CT	Spiral CT	Primary analysis	50	2	7	18
Quaia et al., 2009 [51]	CEUS	Malignant versus benign reader 1	Primary analysis	64	15	8	34
Quaia et al., 2009 [51]	CT	64-row MDCT reader 1	Primary analysis	53	14	19	35
Ding et al., 2021 [52]	CEUS	CEUS LR-5	Primary analysis	170	3	55	45
Ding et al., 2021 [52]	CT/MRI (mixed)	CECT/EOB-MRI LR-5	Primary analysis	188	8	37	40
Mansour et al., 2021 [53]	CEUS	Malignant versus benign	Primary analysis	43	2	3	18
Mansour et al., 2021 [53]	CT	Triphasic CT	Primary analysis	48	4	0	18
Li et al., 2025 [26]	CEUS	CEUS LI-RADS LR-5; nodules <20 mm	Size stratum ≤20 mm	21	0	22	28
Li et al., 2025 [26]	CT/MRI (mixed)	CT/MRI LI-RADS LR-5; nodules <20 mm	Size stratum ≤20 mm	26	2	17	26
Leoni et al., 2010 [42]	CEUS	AASLD criteria; nodules 10-19 mm	Size stratum ≤20 mm	16	1	11	15
Leoni et al., 2010 [42]	CT	AASLD criteria; nodules 10-19 mm	Size stratum ≤20 mm	19	0	8	16
Leoni et al., 2010 [42]	MRI	AASLD criteria; nodules 10-19 mm	Size stratum ≤20 mm	20	1	7	15

TABLE 7: Extracted 2 x 2 contingency data for each included study and imaging test.

One row is shown for each study arm. Primary analysis rows were used for the pooled and head-to-head analyses. Size-stratum rows give the nodule-size strata explicitly reported by two studies without a size restriction and were used, together with the three studies restricted to nodules of ≤20 mm (Forner et al., 2008 [34]; Dai et al., 2008 [36]; and Sangiovanni et al., 2010 [41]), in the ≤20 mm analysis. Indeterminate results were counted as incorrect classifications where this was done in the primary study.

TP, true positive; FP, false positive; FN, false negative; TN, true negative; CEUS, contrast-enhanced ultrasound; CT, computed tomography; CECT, contrast-enhanced CT; MDCT, multidetector CT; MSCT, multislice CT; MRI, magnetic resonance imaging; EOB, gadoxetic acid; Gd, gadolinium; LI-RADS, Liver Imaging Reporting and Data System; LR, LI-RADS category; AASLD, American Association for the Study of Liver Diseases; CHI, contrast harmonic imaging; DTPA, diethylenetriamine pentaacetate; HCC, hepatocellular carcinoma

Table 8 shows the post-test probabilities and predictive values of CEUS, CT, and MRI across pre-test probabilities.

Test	Pre-test probability (%)	Post-test probability after a positive result (PPV, %)	Post-test probability after a negative result (%)	NPV (%)
CEUS	10	49.5	1.7	98.3
CEUS	25	74.6	4.9	95.1
CEUS	50	89.8	13.3	86.7
CEUS	70	95.4	26.3	73.7
CEUS	75	96.4	31.5	68.5
CT	10	41.7	1.7	98.3
CT	25	68.3	4.9	95.1
CT	50	86.6	13.5	86.5
CT	70	93.8	26.7	73.3
CT	75	95.1	31.9	68.1
MRI	10	52.6	2.2	97.8
MRI	25	76.9	6.2	93.8
MRI	50	90.9	16.7	83.3
MRI	70	95.9	31.8	68.2
MRI	75	96.8	37.5	62.5

TABLE 8: Post-test probabilities and predictive values of CEUS, CT, and MRI across pre-test probabilities.

Post-test probabilities were derived from the pooled positive and negative likelihood ratios of each test (CEUS, 8.82 and 0.153; CT, 6.45 and 0.156; MRI, 9.97 and 0.200). The 70% row corresponds to the median prevalence of the target condition in the included CEUS arms; the lower pre-test probabilities represent settings such as incidentally detected lesions. NPV equals 100 minus the post-test probability after a negative result.

CEUS, contrast-enhanced ultrasound; CT, computed tomography; MRI, magnetic resonance imaging; PPV, positive predictive value; NPV, negative predictive value

Additional Information

Author Contributions

All authors have reviewed the final version to be published and agreed to be accountable for all aspects of the work.

Concept and design: Mohamed R. Elazomy

Critical review of the manuscript for important intellectual content: Mohamed R. Elazomy, Wedad A. Kaabi, Aesha A. Hassan, Norah M. Almarzouq, Abdulmalik Meri, Salma A. Tahiri

Supervision: Mohamed R. Elazomy

Acquisition, analysis, or interpretation of data: Wedad A. Kaabi, Aesha A. Hassan, Shahad F. Bagdood, Sheikhah Binmahfooz, Ahmed M. Alzahrani, Norah M. Almarzouq, Abdullah Alhussain, Yazan Daghriri, Layan T. Aldhowayan, Ahad Alhazmi, Abdulmalik Meri, Salma A. Tahiri, Alanood M. Hakami, Dina M. Almasoudi

Drafting of the manuscript: Shahad F. Bagdood, Sheikhah Binmahfooz, Ahmed M. Alzahrani, Abdullah

Alhussain, Yazan Daghriri, Layan T. Aldhowayan, Ahad Alhazmi, Alanood M. Hakami, Dina M. Almasoudi

Disclosures

AI use statement: The authors have declared that no AI tools were used during the work or in the drafting of this article. The authors take full responsibility for the work. **Conflicts of interest:** In compliance with the ICMJE uniform disclosure form, all authors declare the following: **Payment/services info:** All authors have declared that no financial support was received from any organization for the submitted work. **Financial relationships:** All authors have declared that they have no financial relationships at present or within the previous three years with any organizations that might have an interest in the submitted work. **Other relationships:** All authors have declared that there are no other relationships or activities that could appear to have influenced the submitted work.

References

1. Singh BP, Saroha G, Ray R, Mathur V, Mathur A: Characterization of focal liver lesions on contrast enhanced ultrasound. Int J Sci Res. 2023, 12:34-6.
2. Alhyari A, Görg C, Alakhras R, Dietrich CF, Trenker C, Safai Zadeh E: HCC or something else? Frequency of various benign and malignant etiologies in cirrhotic patients with newly detected focal liver lesions in relation to different clinical and sonographic parameters. Diagnostics (Basel). 2022, 12:2079. 10.3390/diagnostics12092079
3. Westwood M, Joore M, Grutters J, et al.: Contrast-enhanced ultrasound using SonoVue® (sulphur hexafluoride microbubbles) compared with contrast-enhanced computed tomography and contrast-enhanced magnetic resonance imaging for the characterisation of focal liver lesions and detection of liver metastases: a systematic review and cost-effectiveness analysis. Health Technol Assess. 2013, 17:1-243. 10.3310/hta17160
4. Piscaglia F, Lencioni R, Sagrini E, Pina CD, Cioni D, Vidili G, Bolondi L: Characterization of focal liver lesions with contrast-enhanced ultrasound. Ultrasound Med Biol. 2010, 36:531-50. 10.1016/j.ultrasmedbio.2010.01.004
5. Phukan P, Boruah DK, Sarma K: Diagnostic accuracy of contrast-enhanced ultrasound in the characterization of focal liver lesions: a prospective study. Glob J Med Pharm Sci. 2026, 4:1-7.
6. Barr RG: Contrast enhanced ultrasound for focal liver lesions: how accurate is it? . Abdom Radiol (NY). 2018, 43:1128-33. 10.1007/s00261-017-1257-6
7. Laugesen NG, Nolsoe CP, Rosenberg J: Clinical applications of contrast-enhanced ultrasound in the pediatric work-up of focal liver lesions and blunt abdominal trauma: a systematic review. Ultrasound Int Open. 2017, 3:E2-7. 10.1055/s-0042-124502
8. Ren X, Li J, Zhang J, Zhan W: Advances in the application of contrast-enhanced ultrasound in the diagnosis and treatment of focal liver lesions (Article in Chinese). J Diagn Concepts Pract. 2022, 21:684-90. 10.16150/j.1671-2870.2022.06.004
9. Mavoori S, Dickson M, Sumit KU, Abhilash A, Kunjumon A: Diagnostic value of contrast enhanced ultrasound (CEUS) compared to standard imaging techniques for evaluation of hepatic lesions: a systematic review. IOSR J Nurs Health Sci. 2024, 13:1-5. 10.9790/1959-1306030105
10. Strobel D, Seitz K, Blank W, et al.: Tumor-specific vascularization pattern of liver metastasis, hepatocellular carcinoma, hemangioma and focal nodular hyperplasia in the differential diagnosis of 1,349 liver lesions in contrast-enhanced ultrasound (CEUS). Ultraschall Med. 2009, 30:376-82. 10.1055/s-0028-1109672
11. Schwarze V, Marschner C, Völckers W, de Figueiredo GN, Rübenthaler J, Clevert DA: The diagnostic performance of contrast-enhanced ultrasound (CEUS) for evaluating hepatocellular carcinoma (HCC) juxtaposed to MRI findings; a retrospective single-center analysis of 292 patients. Clin Hemorheol Microcirc. 2020, 76:155-60. 10.3233/CH-209213
12. von Herbay A, Westendorff J, Gregor M: Contrast-enhanced ultrasound with SonoVue: differentiation between benign and malignant focal liver lesions in 317 patients. J Clin Ultrasound. 2010, 38:1-9. 10.1002/jcu.20626
13. Stavrou GA, Stang A, Raptis DA, et al.: Intraoperative (contrast-enhanced) ultrasound has the highest diagnostic accuracy of any imaging modality in resection of colorectal liver metastases. J Gastrointest Surg. 2021, 25:3160-9. 10.1007/s11605-021-04925-2
14. Page MJ, McKenzie JE, Bossuyt PM, et al.: The PRISMA 2020 statement: an updated guideline for reporting systematic reviews. BMJ. 2021, 372:n71. 10.1136/bmj.n71
15. McInnes MD, Moher D, Thombs BD, et al.: Preferred Reporting Items for a systematic review and meta-analysis of diagnostic test accuracy studies: the PRISMA-DTA statement. JAMA. 2018, 319:388-96. 10.1001/jama.2017.19163
16. Macaskill P, Gatsonis C, Deeks JJ, Harbord RM, Takwoingi Y: Chapter 10: analysing and presenting results. Cochrane Handbook for Systematic Reviews of Diagnostic Test Accuracy. Deeks JJ, Bossuyt PM, Gatsonis C (ed): The Cochrane Collaboration, London, UK; 2010.
17. Cohen J: A coefficient of agreement for nominal scales . Educ Psychol Meas. 1960, 20:37-46. 10.1177/001316446002000104
18. Whiting PF, Rutjes AW, Westwood ME, et al.: QUADAS-2: a revised tool for the quality assessment of diagnostic accuracy studies. Ann Intern Med. 2011, 155:529-36. 10.7326/0003-4819-155-8-201110180-00009
19. The R Project for Statistical Computing . (2026). Accessed: October 29, 2026: https://www.R-project.org/.
20. Reitsma JB, Glas AS, Rutjes AW, Scholten RJ, Bossuyt PM, Zwinderman AH: Bivariate analysis of sensitivity and specificity produces informative summary measures in diagnostic reviews. J Clin Epidemiol. 2005, 58:982-90. 10.1016/j.jclinepi.2005.02.022
21. Rutter CM, Gatsonis CA: A hierarchical regression approach to meta-analysis of diagnostic test accuracy evaluations. Stat Med. 2001, 20:2865-84. 10.1002/sim.942

22. Higgins JP, Thompson SG, Deeks JJ, Altman DG: Measuring inconsistency in meta-analyses . BMJ. 2003, 327:557-60. 10.1136/bmj.327.7414.557
23. Deeks JJ, Macaskill P, Irwig L: The performance of tests of publication bias and other sample size effects in systematic reviews of diagnostic test accuracy was assessed. J Clin Epidemiol. 2005, 58:882-93. 10.1016/j.jclinepi.2005.01.016
24. Fagan TJ: Letter: nomogram for Bayes's theorem. N Engl J Med. 1975, 293:257. 10.1056/NEJM197507312930513
25. Schünemann HJ, Mustafa RA, Brozek J, et al.: GRADE guidelines: 21 part 2. Test accuracy: inconsistency, imprecision, publication bias, and other domains for rating the certainty of evidence and presenting it in evidence profiles and summary of findings tables. J Clin Epidemiol. 2020, 122:142-52. 10.1016/j.jclinepi.2019.12.021
26. Li Y, Li S, Li Q, et al.: Combination of CT/MRI LI-RADS with second-line contrast-enhanced ultrasound using sulfur hexafluoride or perfluorobutane for diagnosing hepatocellular carcinoma in high-risk patients. Korean J Radiol. 2025, 26:346-59. 10.3348/kjr.2024.0980
27. Dumitrescu CI, Gheonea IA, Săndulescu L, Surlin V, Săftoiu A, Dumitrescu D: Contrast enhanced ultrasound and magnetic resonance imaging in hepatocellular carcinoma diagnosis. Med Ultrason. 2013, 15:261-7. 10.11152/mu.2013.2066.154.cd2
28. D'Onofrio M, Crosara S, De Robertis R, Canestrini S, Cantisani V, Morana G, Mucelli RP: Malignant focal liver lesions at contrast-enhanced ultrasonography and magnetic resonance with hepatospecific contrast agent. Ultrasound. 2014, 22:91-8. 10.1177/1742271X13513888
29. Giorgio A, De Stefano G, Coppola C, et al.: Contrast-enhanced sonography in the characterization of small hepatocellular carcinomas in cirrhotic patients: comparison with contrast-enhanced ultrafast magnetic resonance imaging. Anticancer Res. 2007, 27:4263-9.
30. Takahashi M, Maruyama H, Shimada T, Kamezaki H, Sekimoto T, Kanai F, Yokosuka O: Characterization of hepatic lesions (≤ 30 mm) with liver-specific contrast agents: a comparison between ultrasound and magnetic resonance imaging. Eur J Radiol. 2013, 82:75-84. 10.1016/j.ejrad.2012.05.035
31. Wang JY, Feng SY, Yi AJ, et al.: Comparison of contrast-enhanced ultrasound versus contrast-enhanced magnetic resonance imaging for the diagnosis of focal liver lesions using the Liver Imaging Reporting and Data System. Ultrasound Med Biol. 2020, 46:1216-23. 10.1016/j.ultrasmedbio.2020.01.023
32. Seitz K, Bernatik T, Strobel D, et al.: Contrast-enhanced ultrasound (CEUS) for the characterization of focal liver lesions in clinical practice (DEGUM multicenter trial): CEUS vs. MRI--a prospective comparison in 269 patients. Ultraschall Med. 2010, 31:492-9. 10.1055/s-0029-1245591
33. Seitz K, Strobel D, Bernatik T, et al.: Contrast-enhanced ultrasound (CEUS) for the characterization of focal liver lesions - prospective comparison in clinical practice: CEUS vs. CT (DEGUM multicenter trial). Parts of this manuscript were presented at the Ultrasound Dreiländertreffen 2008, Davos. Ultraschall Med. 2009, 30:383-9. 10.1055/s-0028-1109673
34. Forner A, Vilana R, Ayuso C, et al.: Diagnosis of hepatic nodules 20 mm or smaller in cirrhosis: prospective validation of the noninvasive diagnostic criteria for hepatocellular carcinoma. Hepatology. 2008, 47:97-104. 10.1002/hep.21966
35. Clevert DA, Jung EM, Stock KF, Weckbach S, Feuerbach S, Reiser M, Jung F: Evaluation of malignant liver tumors: biphasic MS-CT versus quantitative contrast harmonic imaging ultrasound. Z Gastroenterol. 2009, 47:1195-202. 10.1055/s-0028-1109396
36. Dai Y, Chen MH, Fan ZH, Yan K, Yin SS, Zhang XP: Diagnosis of small hepatic nodules detected by surveillance ultrasound in patients with cirrhosis: comparison between contrast-enhanced ultrasound and contrast-enhanced helical computed tomography. Hepatol Res. 2008, 38:281-90. 10.1111/j.1872-034X.2007.00269.x
37. Li R, Guo Y, Hua X, He Y, Ding J, Guo A, Luo M: Characterization of focal liver lesions: comparison of pulse-inversion harmonic contrast-enhanced sonography with contrast-enhanced CT. J Clin Ultrasound. 2007, 35:109-17. 10.1002/jcu.20310
38. Shiozawa K, Watanabe M, Ikehara T, et al.: Comparison of contrast-enhanced ultrasonograpy with Gd-EOB-DTPA-enhanced MRI in the diagnosis of liver metastasis from colorectal cancer. J Clin Ultrasound. 2017, 45:138-44. 10.1002/jcu.22421
39. Burrowes DP, Medellin A, Harris AC, Milot L, Lethebe BC, Wilson SR: Characterization of focal liver masses: a multicenter comparison of contrast-enhanced ultrasound, computed tomography, and magnetic resonance imaging. J Ultrasound Med. 2021, 40:2581-93. 10.1002/jum.15644
40. Hu J, Burrowes DP, Caine BA, et al.: Nodules identified on surveillance ultrasound for HCC: CEUs or MRI as the initial test?. J Ultrasound Med. 2023, 42:1181-90. 10.1002/jum.16183
41. Sangiovanni A, Manini MA, Iavarone M, et al.: The diagnostic and economic impact of contrast imaging techniques in the diagnosis of small hepatocellular carcinoma in cirrhosis. Gut. 2010, 59:638-44. 10.1136/gut.2009.187286
42. Leoni S, Piscaglia F, Golfieri R, Camaggi V, Vidili G, Pini P, Bolondi L: The impact of vascular and nonvascular findings on the noninvasive diagnosis of small hepatocellular carcinoma based on the EASL and AASLD criteria. Am J Gastroenterol. 2010, 105:599-609. 10.1038/ajg.2009.654
43. Blondin D, Erhardt A, Crynen K, et al.: Diagnosis of focal liver lesions in cirrhotic patients: comparison of contrast-enhanced ultrasound using sulphur hexafluoride (SF6) microbubbles and MRI using Gd-EOB-DTPA (Article in German). Z Gastroenterol. 2011, 49:23-9. 10.1055/s-0029-1245781
44. Trillaud H, Bruel JM, Valette PJ, et al.: Characterization of focal liver lesions with SonoVue-enhanced sonography: international multicenter-study in comparison to CT and MRI. World J Gastroenterol. 2009, 15:3748-56. 10.3748/wjg.15.3748
45. Sawatzki M, Meyenberger C, Brand S, Semela D: Contrast-enhanced ultrasound (CEUS) has excellent diagnostic accuracy in differentiating focal liver lesions: results from a Swiss tertiary gastroenterological centre. Swiss Med Wkly. 2019, 149:w20087. 10.4414/smw.2019.20087
46. Gnanasigamani S, Chellathurai A, Priya, Sivakumar, Karthikrajan: Diagnostic accuracy of contrast enhanced ultrasonography in focal liver lesions detected by contrast enhanced computed tomography. Int J Sci Res.

2020, 9:45-9.
47. Ryu SW, Bok GH, Jang JY, et al.: Clinically useful diagnostic tool of contrast enhanced ultrasonography for focal liver masses: comparison to computed tomography and magnetic resonance imaging. Gut Liver. 2014, 8:292-7. 10.5009/gnl.2014.8.3.292
48. Beyer LP, Wassermann F, Pregler B, et al.: Characterization of focal liver lesions using CEUS and MRI with liver-specific contrast media: experience of a single radiologic center. Ultraschall Med. 2017, 38:619-25. 10.1055/s-0043-105264
49. Quaia E, D'Onofrio M, Palumbo A, Rossi S, Bruni S, Cova M: Comparison of contrast-enhanced ultrasonography versus baseline ultrasound and contrast-enhanced computed tomography in metastatic disease of the liver: diagnostic performance and confidence. Eur Radiol. 2006, 16:1599-609. 10.1007/s00330-006-0192-7
50. Catala V, Nicolau C, Vilana R, Pages M, Bianchi L, Sanchez M, Bru C: Characterization of focal liver lesions: comparative study of contrast-enhanced ultrasound versus spiral computed tomography. Eur Radiol. 2007, 17:1066-73. 10.1007/s00330-006-0444-6
51. Quaia E, Alaimo V, Baratella E, Medeot A, Midiri M, Cova MA: The added diagnostic value of 64-row multidetector CT combined with contrast-enhanced US in the evaluation of hepatocellular nodule vascularity: implications in the diagnosis of malignancy in patients with liver cirrhosis. Eur Radiol. 2009, 19:651-63. 10.1007/s00330-008-1179-3
52. Ding J, Long L, Zhang X, et al.: Contrast-enhanced ultrasound LI-RADS 2017: comparison with CT/MRI LI-RADS. Eur Radiol. 2021, 31:847-54. 10.1007/s00330-020-07159-z
53. Mansour MG, Kader MH, Arafa HM, Ali SA: Characterization of focal liver lesions using sulphur hexafluoride (SF6) microbubble contrast-enhanced ultrasonography. Egypt J Radiol Nucl Med. 2021, 52:7. 10.1186/s43055-020-00374-0
54. Soussan M, Aubé C, Bahrami S, Boursier J, Valla DC, Vilgrain V: Incidental focal solid liver lesions: diagnostic performance of contrast-enhanced ultrasound and MR imaging. Eur Radiol. 2010, 20:1715-25. 10.1007/s00330-009-1700-3
55. Yang Q, Zheng R, Zhou J, et al.: On-site diagnostic ability of CEUS/CT/MRI for hepatocellular carcinoma (2019-2022): a multicenter study. J Ultrasound Med. 2023, 42:2825-38. 10.1002/jum.16321
56. Huang H, He DN, Lu RF, et al.: The role of contrast-enhanced ultrasound in the radiological classification of liver observations identified by CT and MRI. Radiol Med. 2025, 130:805-16. 10.1007/s11547-025-01995-z